Engineering 28 (2023) 206–221

Contents lists available at ScienceDirect

Engineering

journal homepage: www.elsevier.com/locate/eng

Research
Medical Engineering—Article

Discovery of Kaempferol, a Novel ADAM10 Inhibitor, as a Potential Treatment for *Staphylococcus aureus* Infection

Tingting Wang [a,b,#], Jianfeng Wang [a,b,c,#], Xiangzhu Xu [b], Fan Jiang [b], Hongfa Lv [b], Qinghui Qi [b], Can Zhang [b], Qianghua Lv [d,*], Xuming Deng [a,b,*]

[a] *Department of Respiratory Medicine, Center for Pathogen Biology and Infectious Diseases & Key Laboratory of Organ Regeneration and Transplantation of the Ministry of Education, State Key Laboratory for Zoonotic Diseases, The First Hospital of Jilin University, Changchun 130021, China*
[b] *State Key Laboratory for Diagnosis and Treatment of Severe Zoonotic Infectious Diseases & Key Laboratory of Zoonosis Research, Ministry of Education, Institute of Zoonosis, College of Veterinary Medicine, Jilin University, Changchun 130062, China*
[c] *Key Laboratory for Molecular Enzymology and Engineering of Ministry of Education, School of Life Sciences, Jilin University, Changchun 130012, China*
[d] *Key Laboratory of Livestock and Poultry Multi-omics of MARA & Shandong Key Laboratory of Animal Disease Control and Breeding, Institute of Animal Science and Veterinary Medicine, Shandong Academy of Agricultural Sciences, Jinan 250100, China*

ARTICLE INFO

Article history:
Received 18 October 2022
Revised 19 February 2023
Accepted 23 March 2023
Available online 14 April 2023

Keywords:
Host-directed therapy
Kaempferol
ADAM10 inhibitor
Staphylococcus aureus infection
Barrier disruption
Necroptosis

ABSTRACT

Host-directed therapy (HDT) is an emerging novel approach for treating multidrug-resistant *Staphylococcus aureus* (*S. aureus*) infection. Functioning as the indispensable specific cellular receptor for α-toxin (Hla), a-disintegrin and metalloproteinase 10 (ADAM10) is exploited to accelerate *S. aureus* infection through diverse mechanisms. The extraordinary contribution of ADAM10 to *S. aureus* pathogenesis renders it an attractive HDT target for combating *S. aureus* infection. Our study is the first to demonstrate the indispensable role of ADAM10 in *S. aureus*-induced necroptosis, and it enhances our knowledge of the role of ADAM10 in *S. aureus* infection. Using a fluorogenic substrate assay, we further identified kaempferol as a potent ADAM10 inhibitor that effectively protected mice from *S. aureus* infection by suppressing Hla-mediated barrier disruption and necroptosis. Collectively, our work presents a novel host-directed therapeutic strategy for using the promising candidate kaempferol to treat *S. aureus* infection and other diseases relevant to the disordered upregulation of ADAM10.

1. Introduction

The increasing emergence of multidrug-resistant *Staphylococcus aureus* (*S. aureus*; MDRSA), especially methicillin-resistant *S. aureus* (MRSA), has seriously threatened public health worldwide under the global antibiotic crisis. Except for the few antimicrobial drugs under development, novel alternative therapeutic approaches are urgently needed. Among these approaches, host-directed therapy (HDT) stands out for its superiority in that it is less prone to inducing resistance. This HDT-based strategy is designed to prevent infection through blocking the interaction between bacterial factors and host factors, hindering key host mechanisms, targeting cellular pathways that are perturbed by bacterial or virulence factors, or rebalancing the disordered responses at the site of the pathology, rather than targeting bacterial viability [1,2]. Although HDT drugs are considered difficult to stand alone, the combination of the HDT approach with traditional antibiotics will significantly reduce antibiotic treatment failures, which is particularly important for the treatment of antibiotic-resistant infections.

S. aureus has successfully evolved a plenty of virulence determinants to facilitate survival in the microenvironment encountered during infection and to interact with host cells or molecules, which enable the bacteria to breach host structural and immunological barriers. Among these essential virulence factors, α-toxin (Hla) represents the most pivotal and best-characterized pore-forming toxin (PFT) secreted by *S. aureus*, participating in pathogenesis through multifaceted mechanisms during different diseases, including pneumonia, sepsis, and skin infection [3]. After nearly a century of research on Hla, the first specific cellular high-affinity

* Corresponding authors.
E-mail addresses: lvqianghua129@jlu.edu.cn (Q. Lv), Dengxm@jlu.edu.cn (X. Deng).
[#] These authors contributed equally to this work.

https://doi.org/10.1016/j.eng.2023.03.006

receptor for Hla was genetically identified [4]. Functioning as an indispensable mediator for the pore formation of Hla, a-disintegrin and metalloproteinase 10 (ADAM10) is required for Hla to cause cytotoxicity and accelerate Hla-dependent pathogenesis of *S. aureus* infection in the host. Genome-wide clustered regularly interspaced short palindromic repeats (CRISPR) screening further determines the specificity and indispensability of ADAM10 for Hla-mediated cytotoxicity [5]. Strikingly, Hla pore formation in turn stimulates a rapid upregulation of the metalloprotease activity of ADAM10, which triggers the proteolytic processing of classical adhesion molecules in the cadherin family, including epithelial (E)-cadherin and vascular endothelial (VE)-cadherin, thereby leading to severe barrier dysfunction that benefits bacterial expansion during *S. aureus* infection [6,7]. In addition, the interaction of Hla and ADAM10 alters integrin-mediated cell signaling events, causing the rapid dephosphorylation of focal adhesion kinase (FAK), paxillin, proto-oncogene tyrosine-protein kinase (Src), and 130 kDa Crk-associated substrate (p130Cas), a cellular event defined as the second molecular mechanism by which Hla further disrupts the cell layer and tissue barrier by inducing the dissolution of focal adhesions [4]. Notably, the activation of ADAM10 by Hla also results in the cleavage of acid sphingomyelinase in internalized vesicles, which is closely connected to the degradation of tight junctions in epithelial cells or endothelial cells [8]. Barrier breakdown in epithelial or endothelial cells is a critical pathogenesis that promotes the spread of infection during the initial state of invasive infection. Thus, ADAM10 represents a promising target for HDT-based approaches to prevent *S. aureus* infections by preventing barrier disruption.

In addition to the cadherin family, zinc-dependent catalysis by ADAM10 leads to the activation of intracellular signaling pathways and the release of functional soluble ectodomains that modulate immunity and other cell events critical for developmental signaling and pathological processes [9,10]. Tumor necrosis factor (TNF)-induced necroptosis, a mode of caspase-independent and highly proinflammatory programmed cell death regulated by receptor-interacting serine–threonine kinase 1 (RIP1) and RIP3 and executed by the pore-forming element known as mixed lineage kinase domain-like (MLKL) [11,12]. A recent study showed that Hla-induced necroptosis is a major mechanism of *S. aureus* lung damage, which leads to the impaired clearance of *S. aureus* and severe inflammatory pathology during *S. aureus* infection [13]; however, the participation of ADAM10 enzymatic activity in Hla-mediated necroptosis remains unknown. Given the direct involvement of Hla in upregulating ADAM10 activity and *S. aureus*-induced necroptosis, ADAM10 may also accelerate Hla-mediated cytotoxicity by modulating the TNF-induced necroptosis pathway, which should be further validated.

Kaempferol (3,4,5,7-tetrahydroxyflavone) is a natural polyphenolic that is abundant in vegetables and fruits as well as many types of herbs that have been widely used in Chinese medicines. This natural small molecule possesses a wide range of therapeutic properties, such as antioxidant, anticancer, and neuroprotective activities, and it also regulates T-cell functions [14]. Although previous studies have extensively characterized the drug action of kaempferol in different cases, no research has reported the effect of kaempferol on the ADAM10-associated pathogenesis of *S. aureus*. In the present study, we report a new role of ADAM10 enzymatic activity in *S. aureus*-induced necroptosis. Moreover, we present kaempferol as a potent ADAM10 inhibitor that abrogated the dramatic upregulation of ADAM10 metalloprotease activity boosted by Hla. Accordingly, Hla/ADAM10-mediated barrier disruption was strongly suppressed. Further study demonstrated that *S. aureus*-induced necroptosis and necroptosis-associated inflammatory responses were also blocked by kaempferol. *In vivo*, kaempferol treatment effectively protected mice from lethal pneumonia and mastitis caused by *S. aureus*. In summary, the findings in our work preliminarily elucidated the function of ADAM10 in *S. aureus*-induced necroptosis and identified the natural compound kaempferol as an inhibitor of ADAM10, which proved to have great potential to hinder *S. aureus* infections or perhaps other diseases related to the upregulation of ADAM10.

2. Material and methods

2.1. Reagents and antibodies

Kaempferol (> 98%) purchased from Herbpurify (China) was dissolved in dimethyl sulfoxide (DMSO; Sigma-Aldrich, USA) to make a 20 $mg{\cdot}mL^{-1}$ stock solution that was stored at –20 °C. For *in vitro* assays, the cells were all pretreated with kaempferol 3 h prior to experimentation. For *in vivo* studies, 100 $mg{\cdot}kg^{-1}$ kaempferol was delivered to the mice via subcutaneous route 8 h prior to infection and then administered every 8 h. Fluorogenic peptide substrate (Mca-PLAQAV-Dpa-RSSSR-NH2; R&D Systems, USA) was supplied as a stock solution at a concentration of 10 $mmol{\cdot}L^{-1}$ in DMSO. Ionomycin purchased from Sigma-Aldrich was dissolved in sterilized water to make a 5 $mmol{\cdot}L^{-1}$ stock solution. Evans blue dye (Cat#E2129; Sigma-Aldrich) was dissolved in sterilized phosphate-buffered saline (PBS) to make a 2% (w/v) solution. Live/dead reagent (Invitrogen, USA) and a Cytotoxicity Detection Kit (Roche, Switzerland) were used to evaluate cell death. T-PER Tissue Protein Extraction Reagents (Thermo Scientific, USA) and a Pierce™ BCA Protein Assay Kit (Thermo Scientific) were used to extract the total protein and determine the concentration of obtained protein, respectively. DiD cell-labeling solution (Cat#C1039; Beyotime Biotechnology, China) was used to probe the cell membrane for immunofluorescence microscopy analysis.

The antibodies used in this study were listed as follows: mouse anti-human E-cadherin antibody (Cat#610182) against the C-terminal domain of the protein was purchased from BD Biosciences (USA) for immunoprecipitation and western blot assay; rabbit anti-human E-cadherin antibody (Cat#20874-1-AP) used for immunofluorescence microscopy analysis was purchased from Proteintech (USA); a Necroptosis Antibody Sample Kit (Cat#98110T) purchased from Cell Signaling Technology (USA) was used to analyze the necroptosis pathway; rabbit anti-MLKL antibody (Cat#ab184718) used for immunofluorescence microscopy analysis was purchased from Abcam (UK); rabbit anti-c-Jun N-terminal kinase (JNK) antibody (Cat#51151-1-AP), rabbit anti-extracellular signal regulated kinase (ERK) antibody (Cat#51068-1-AP) and mouse anti-β-actin antibody (Cat#66009-1-Ig) were purchased from Proteintech; rabbit anti-phosphor-stress-activated protein kinase (SAPK)/JNK (Thr183(221) + Thr185(223)) (Cat#ARG51807), rabbit anti-phospho-ERK1/2 (Thr202/Thr204) (Cat#ARG52277), rabbit anti-phospho-nuclear factor kappa-B (NF-κB) kinase (IKK) alpha (Thr23) (Cat#ARG51630), and rabbit anti-IKK alpha (Cat#ARG65746) were purchased from Arigo (China); rabbit antibody against NF-κB p65 (Cat#8242), phospho-NF-κB p65 (Ser536) (Cat#3033S), p38 mitogen-activated protein kinase (MAPK) (Cat#8690), and phospho-p38 MAPK (Thr180/Thr182) (Cat#4511S) were purchased from Cell Signaling Technology. Horseradish peroxidase (HRP)-conjugated anti-mouse immunoglobulin G (IgG) (Cat#146 SA00001-1) and anti-rabbit (Cat#SA00001-2) antibodies were purchased from Proteintech. Alexa 488-conjugated secondary antibody (Cat#ab150077) used for immunofluorescence microscopy analysis was purchased from Abcam. Mouse interleukine (IL)-1β, IL-6, and TNF-α enzyme-linked immunosorbent assay (ELISA) kits were purchased from Biolegend (USA), and human IL-1β ELISA kits were purchased from Invitrogen.

2.2. Bacterial strains, cell lines, and culture conditions

MRSA USA300 was obtained from the American Type Culture Collection (ATCC; USA). Wild-type *S. aureus* strain NTCC 8325-4 (wt *S. aureus*) and its *hla*-deficient mutant strain (*Δhla S. aureus*) were a kind gift from Professor Timothy J. Foster (Department of Microbiology, Moyne Institute of Preventive Medicine Trinity College, Dublin, Ireland). All the *S. aureus* strains were grown in tryptic soy broth (TSB) broth with shaking at 37 °C. Human alveolar epithelial A549 cells and murine fibroblast L929 cells were cultured in Dulbecco's Modified Eagle Medium (DMEM; Gibco, USA) supplemented with 10% fetal bovine serum (FBS) and 1% penicillin/streptomycin in a 37 °C incubator with 5% CO_2. Human myeloid leukemia monocytes (THP-1 cells) were grown in Roswell Park Memorial Institute (RPMI) 1640 Medium (Gibco) supplemented with 10% FBS and 1% penicillin/streptomycin. To differentiate the THP-1 cells into macrophage-like cells, the cells were cultured with 1 μmol·L^{-1} phorbol 12-myristate 13-acetate (PMA) for 24 h and further grown in weaning medium without antibiotics and PMA for another 24 h. Mouse peritoneal macrophages (MPMs) and bone marrow-derived macrophages (BMDMs) from C57BL/6 mice were obtained as previously described and cultured in RPMI 1640 supplemented with 10% FBS [15,16]. Unless otherwise indicated, the cells were pretreated with the indicated concentration of kaempferol or DMSO vehicle 3 h prior to experimentation throughout the study.

2.3. Susceptibility assay

The minimum inhibitory concentration (MIC) of kaempferol on *S. aureus* strains was determined by the broth microdilution method [17], and the minimum concentration that inhibited *S. aureus* was defined as the MIC. The growth curves of *S. aureus* were monitored by measuring the absorbances at an optical density at 600 nm (OD_{600}) over 30 min intervals until the cultures reached stationary phase.

2.4. Intracellular survival assay

The intracellular assay was performed as previously described [18]. In brief, THP-1 cells were plated in 24-well plates at a density of 8×10^5 cells per well and differentiated with PMA 24 hours prior to infection. After pretreatment with 32 μg·mL^{-1} kaempferol or DMSO vehicle, the cells were washed three times with PBS and infected with *S. aureus* at a multiplicity of infection (MOI) of 20 for 1 h. Next, the cells were washed three times with PBS and then further incubated with lysostaphin (10 μg·mL^{-1}) and gentamicin (200 μg·mL^{-1}) for 1 h to kill extracellular bacteria. Then, the cells were washed again and cultured in 10% RPMI containing gentamicin. At the indicated time points, the cells were washed three times with PBS and lysed with 0.1% Triton X-100, and the bacterial count was determined by microbiological plating.

2.5. Cell transfection

The commercially available small interfering RNAs (siRNAs) used in our study were all obtained from Santa Cruz Biotechnology (USA) and transiently transfected into cells using Lipofectamine® RNAiMAX Reagent (Invitrogen) according to the manufacturer's instructions. The experiments were performed 48 h after transfection.

2.6. Cell-based metalloprotease assay

A549 cells were grown in 96-well plates at 2×10^4 cells per well 24 h prior to experimentation. Cells pretreated with the indicated concentrations of kaempferol ranging from 4 to 32 μg·mL^{-1} or DMSO vehicle were then washed three times with warm PBS and stimulated with 20 μg·mL^{-1} Hla or PBS in serum-free DMEM for 10 min at 37 °C. Following three washes with 25 mmol·L^{-1} Tris buffer (pH 8.0), 10 μmol·L^{-1} fluorogenic peptide substrate was added for a 20 min incubation. Then, the fluorescence intensity was measured on a Tecan Microplate Reader (Mannedorf, Switzerland) with excitation at 320 nm and emission at 405 nm.

2.7. Molecular docking

A molecular docking study was performed to investigate the binding mode between kaempferol and ADAM10 using AutoDock Vina 1.1.2 [19]. The X-ray structure of the ectodomain of ADAM10 (6BE6) was downloaded from the Protein Data Bank (rcsb.org), and the three-demensional (3D) structure of kaempferol was downloaded from ChemBioDraw Ultra 14.0.

2.8. Measurement of A549 monolayer transepithelial electrical resistance (TEER) and permeability

A549 cells were seeded in Corning Transwell permeable supports (24 mm Transwell with 0.4 μm pore polycarbonate membrane inserts) at 6×10^5 cells per well and cultured at 37 °C with 5% CO_2 until the monolayer resistance reached approximately 600 Ω. At the day of the assay, cells pretreated with kaempferol or DMSO vehicle were washed with warm PBS and then induced with 50 μg·mL^{-1} Hla or PBS dispensed in serum-free DMEM in the presence of the indicated concentrations of kaempferol or DMSO vehicle. Concurrently, sodium fluorescein was added to each insert compartment at a final concentration of 10 μg·mL^{-1} to assess the integrity of the A549 monolayer in parallel. The TEER was measured using an epithelial volt–ohm meter (Millicell ERS-2; Millipore, USA) at one-hour intervals, and 100 μL of medium was taken from the basal compartment and deposited in a 96-well plate at each time point. Notably, equal amounts of DMEM were added back every time. The fluorescence intensity was measured using a Tecan Microplate Reader with excitation at 460 nm and emission at 520 nm.

2.9. Immunoprecipitation assay

To analyze the cleavage of E-cadherin by ADAM10 in A549 cells, the cells were grown in six-well plates at 1×10^6 cells per well overnight. The cells pretreated with the indicated concentrations of kaempferol or DMSO vehicle were washed three times with warm PBS and stimulated with 50 μg·mL^{-1} recombinant Hla or PBS dispensed in serum-free DMEM containing kaempferol or DMSO vehicle for 1 h in a CO_2 incubator. Additionally, ionomycin, an agonist of ADAM10 [20], was also applied to illustrate the inhibitory effect of kaempferol on the ADAM10-mediated cleavage of E-cadherin, in which the pretreated cells were incubated with 5 μmol·L^{-1} ionomycin or DMSO in the presence of kaempferol or DMSO vehicle for 1 h. After induction, the cell monolayers were washed with PBS and lysed with 1.5 mL of Nonidet P-40 (NP-40) lysis buffer (150 mmol·L^{-1} NaCl, 10 mmol·L^{-1} Tris, 1 mmol·L^{-1} ethylenediaminetetraacetic acid (EDTA), 0.5% NP-40, and 5% glycerol, pH 7.4) containing protease inhibitor (Roche). Whole-cell lysates from which cellular debris was removed by centrifugation were incubated with anti-C-terminal E-cadherin antibody with rotation for 2 h at 4 °C. Prewashed protein A/G plus agarose (Thermo Scientific) was added to each tube, and the tubes were then rotated at 4 °C overnight. Beads coupled with the immune complex were washed three times with NP-40 buffer and then resuspended in 2 × Laemmli sample buffer, followed by heating denaturation at 95 °C for 8 min. Immunoprecipitated proteins were

separated by on a 4%–10% sodium dodecyl sulfate polyacrylamide gel electrophoresis (SDS-PAGE) gel and probed with anti-C-terminal E-cadherin antibody. The image results were obtained using an enhanced chemiluminescence (ECL) Plus Western Blotting Detection System (Tanon, China).

2.10. Immunofluorescence microscopy analysis

To examine E-cadherin cleavage by immunofluorescence, A549 cells were cultured overnight in glass-bottom cell culture dishes (20 mm) at 5×10^5 cells per well. Following pretreatment with 32 $\mu g \cdot mL^{-1}$ kaempferol or DMSO vehicle, the cells were washed three times with PBS and stimulated with 50 $\mu g \cdot mL^{-1}$ Hla in serum-free DMEM with or without 32 $\mu g \cdot mL^{-1}$ kaempferol for 1 h. Next, the cells were fixed with 4% paraformaldehyde in PBS at room temperature for 10 min, permeabilized with 0.2% Triton X-100 for another 10 min, washed three times with PBS and blocked with 1% bovine serum albumin in PBS containing 0.1% Tween 20 for 1 h at room temperature [21]. Generally, the cells were stained overnight with a human E-cadherin antibody that recognized the extracellular domain (1:100 dilution) at 4 °C, followed by incubation with Alexa Fluor 488-conjugated goat anti-rabbit antibody (1:1000 dilution). After three washes with PBS, the cells were counterstained with Antifade Mounting Medium with 4′,6-diamidino-2-phenylindole (DAPI) (Beyotime Biotechnology) to probe the nuclei. Image capture was performed using a laser scanning confocal microscope (Olympus, Japan). To detect the MLKL location in THP-1 cells infected with *S. aureus* at an MOI of 20 for 6 h with different treatments, live cells were stained with the DiD cell-labeling probe before fixation. The following steps were the same as those described above except for the primary antibody.

2.11. Cytotoxicity assays

To analyze the cytotoxicity caused by *S. aureus*, THP-1 cells were grown in 96-well plates at 1×10^5 cells per well, and MPMs and A549 cells were seeded into 96-well plates at 1×10^5 cells and 2×10^4 cells per well, respectively. On the day of the assay, the indicated concentrations of kaempferol or DMSO vehicle were added to cells 3 h prior to infection. Then, bacterial suspensions in cell medium were added to the cells at designated MOI with kaempferol for further infection. After the indicated infection duration, lactate dehydrogenase (LDH) release into the co-culture supernatant was assessed with a Cytotoxicity Detection Kit according to the manufacturer's instructions, and the cells in the bottom were stained with live/dead reagent containing both membrane-impermeable (red) and membrane-permeable (green) fluorescent dyes. The visualized results were obtained using an inverted fluorescence microscope (Olympus).

To analyze TNF-induced necroptosis, L929 cells were cultured overnight in 96-well plates at 5×10^4 cells per well followed by pretreatment with the indicated concentrations of kaempferol or vehicle prior to induction. Necroptosis was then stimulated using a Necroptosis Inducer Kit with TSZ (Beyotime Biotechnology), which consists of TNF-α, second mitochondria-derived activator of caspase (SMAC) mimetic (SM-164), and benzyloxycarbonyl-Val–Ala–Asp-fluoromethyl ketone (Z-VAD-FMK), in the presence of kaempferol or vehicle. After 18 h of induction, cell death was determined by measuring the LDH release using a Cytotoxicity Detection Kit according to the manufacturer's instructions. Subsequently, the cells in the bottom were stained with an Apoptosis and Necrosis Assay Kit containing Hoechst and Propidium Iodide (PI) dyes (Beyotime Biotechnology), and the results were visualized using a fluorescence microscope.

For analysis of lipopolysaccharide (LPS)-induced necroptosis with the Cytotoxicity Detection Kit and to counterstain with Hoechst and PI, differentiated BMDMs pretreated with kaempferol or vehicle were induced by 10 $\mu mol \cdot L^{-1}$ benzyloxycarbonyl-Val–Ala–Asp (Z-VAD) and designated concentrations of LPS (*Escherichia coli* O26:B6; Sigma-Aldrich) for 24 h. LDH release assays and fluorescence microscopy analysis were carried out as described above.

2.12. ELISA analysis

The IL-1β concentrations in the THP-1 culture supernatants were measured with human IL-1β ELISA kits according to the manufacturer's protocol. The IL-1β, TNF-α, and IL-6 in mouse tissue homogenates were assessed using a mouse ELISA MAX Deluxe Set (Biolegend).

2.13. Immunoblot analysis

THP-1 cells infected with *S. aureus* at an MOI of 20 for 6 h with different treatments were washed with PBS and lysed using T-PER Tissue Protein Extraction Reagents followed by centrifugation at 10 000*g* for 8 min. The total protein concentration of each sample was determined using a Pierce™ BCA Protein Assay Kit. Biological samples in sodium dodecyl sulfate (SDS) buffer were separated by 4%–10% SDS-PAGE, transferred to polyvinylidene difluoride membranes using a semidry electrophoretic system (Bio-Rad, USA) and blocked with 5% skimmed milk in tris buffered saline with Tween 20 (TBST) for 2 h at room temperature. The immunoblots were detected using standard methods with primary antibodies against protein targets of interest, followed by incubation with HRP-conjugated secondary antibodies. The immunoblots were developed with the enhanced chemiluminescence ECL kit (Biosharp, China) and visualized using an ECL Plus Western Blotting Detection System. The integrated density of each western blot band was quantified using Image-Pro software and normalized to β-actin.

2.14. RNA isolation and quantitative real-time polymerase chain reaction (qRT-PCR)

Total RNA isolation was performed as described previously [22], and the primer pairs used for qRT-PCR are listed in Table 1. qRT-PCR was performed on an Applied Bioscience 7500 thermocycler using FastStart Universal SYBR Green Master Mix (Roche). The cycling parameters were an initial denaturation step at 95 °C for 30 s, followed by 40 cycles of 95 °C for 15 s, and 60 °C for 1 min. RNA expression was normalized to glyceraldehyde-3-phosphate dehydrogenase (*GAPDH*) as a reference gene, and the changes in gene transcription were calculated using the $2^{-\Delta\Delta CT}$ method.

2.15. Miles assay and mouse infection analysis

C57BL/6 female mice and BALB/c female mice aged 6–8 weeks were purchased from Liaoning Changsheng Biotechnology Co., Ltd. (China). They received humane care under standard laboratory housing conditions (specific pathogen-free, 12-h light/dark cycle, 55% humidity and (25 ± 1) °C) in individually ventilated cages (IVCs) with soft bedding. The mice were subcutaneously injected with vehicle or a single dose of 100 $mg \cdot kg^{-1}$ kaempferol at the indicated times, and drug delivery was maintained at 8 h intervals.

To assess the effect of kaempferol on Hla-induced endothelial barrier disruption *in vivo*, the BALB/c mice were subcutaneously injected with 7.5 μg of endotoxin-free recombinant Hla in 100 μL of PBS followed by the intravenous delivery of 100 μL of 2% Evans blue dye (w/v) in sterilized PBS 3 h later. The mice were then anesthetized with 5% isoflurane and killed by rapid cervical dislocation

Table 1
Sequence of primers used for qRT-PCR assays.

Gene	Primer	Sequence (5′–3′)
Human *GAPDH*	Sense	GGGGAAGGTGAAGGTCG
	Anti-sense	TGGAAGATGGTGATGGGAT
Human *IL-1β*	Sense	AGATGGCTTATTACAGTGGCAA
	Anti-sense	AGTGGTGGTCGGAGATTCG
Human *IL-6*	Sense	GTAGTGAGGAACAAGCCAGAGC
	Anti-sense	CTACATTTGCCGAAGAGCC
Human *TNF-α*	Sense	CCAGGCGGTGCTTGTTC
	Anti-sense	GGCTACAGGCTTGTCACTCG
Human *CXCL1*	Sense	GGGGAAGGTGAAGGTCG
	Anti-sense	TGGAAGATGGTGATGGGAT
Human *ADAM10*	Sense	ACCTCAAGAAGAACATGCTGCTA
	Anti-sense	CGGAGAAGTCTGTGGTCTGGTA

GAPDH: glyceraldehyde-3-phosphate dehydrogenase; CXCL1: C–X–C motif chemokine ligand 1.

30 min later. Evans blue dye extravasation from the vasculature into the excised skin was quantified by formamide extraction (65 °C, 24 h) and spectrophotometrically detected at OD_{620}. In addition, their skin tissues were fixed in 10% formalin (w/v) and stained with hematoxylin and eosin (H&E) to assess the lesions under a microscope.

MRSA USA300, a highly virulent epidemic methicillin-resistant strain, and NTCC 8325–4, a standard laboratory strain, were used to establish lethal *S. aureus* pneumonia. Fifty milliliter subculture aliquots of USA300 and NTCC 8325–4 (OD_{600} = 0.6) were centrifuged (4500*g*, 8 min), washed three times and resuspended in 5 mL of PBS and 1.5 mL of PBS, respectively. C57BL/6 mice pretreated with a single dose of 100 $mg \cdot kg^{-1}$ kaempferol or vehicle were inoculated with 2×10^8 colony-forming unit (CFU) MRSA USA300 or 6×10^8 CFU NTCC 8325-4 by delivering 30 μL of those suspensions via the intranasal route. The mortality of the mice was recorded until 72 h after infection. For other analyses, the mice were challenged with 1×10^8 CFU USA300 bacteria and then anesthetized at 24 h post-infection as described above. Bronchoalveolar lavage (BAL) was performed according to a previous study [23], and the BAL fluids (BALF) were subjected to an examination of total cell infiltration and protein exudation. Additionally, the concentrations of cytokines in the BALF were measured using ELISA kits according to the manufacturer's instructions. To perform the bacterial burden assay, histopathology analysis, myeloperoxidase (MPO) detection and wet/dry weight ratio measurement, the infected mice were anesthetized at 24 h post-infection. Then, the left lungs were fixed in 10% formalin (w/v) and stained with H&E to examine the histopathologic injury under a microscope. Accordingly, the remaining lung tissues were homogenized in PBS (10% w/v) to analyze the bacterial burden by microbiological plating. In addition, the MPO activity and wet/dry weight ratios of the lungs were also assessed.

Lactating BALB/c mice were used 7 d after the birth of their offspring to establish a mouse mastitis model with an intraductal inoculation of MRSA USA300 as recently reported [24]. In brief, on the day of the experiment, the offspring were weaned 2 h before bacterial inoculation, the mice were anesthetized with 5% isoflurane, and their teats were disinfected with 75% ethanol. The orifices of both the R4 (on the right) and L4 (on the left) glands of the fourth abdominal mammary gland pair were exposed through a slight cut near the end of the teat. Next, 50 μL of bacterial suspension containing 5×10^6 CFU USA300 was slowly injected through the teat canal using a syringe with a 3-gauge blunt needle. The mice were sacrificed at 24 h post-infection to harvest the mammary glands. The tissues were homogenized in sterile PBS (10% w/v) to assess the bacterial burden and inflammatory cytokines. In addition, the mammary tissues were also fixed in 10% formalin and stained with H&E for histopathological examination.

2.16. Statistical analysis

All the data analyses were performed using GraphPad Prism 5.0 (USA). The numeric data from no less than three independent experiments are presented as mean ± standard error of mean (SEM). The statistical significance between two independent groups was determined by unpaired two-tailed Student's *t* test. Comparisons among more than two groups were tested using one-way analysis of variance (ANOVA) followed by Bonferroni's post hoc test, and the post hoc test was performed only if F achieved $P < 0.05$ with no significant variance in homogeneity. The mouse survival rate was analyzed using the log-rank (Mantel-Cox) test. *: $P < 0.05$ and **: $P < 0.01$.

2.17. Study approval

All the animal experiments were approved by the Animal Welfare and Research Ethics Committee at Jilin University (No. ALKT202104003) and were strictly conducted in compliance with the relevant guidelines determined by this committee.

3. Results

3.1. Kaempferol inhibited ADAM10-mediated barrier disruption by abrogating Hla-triggered rapid upregulation of ADAM10 metalloprotease activity

Given the critical role of ADAM10 in *S. aureus* pathogenesis, we performed cell-based metalloprotease assays to identify the effective inhibitors of ADAM10 from a natural compound library established in our laboratory (Fig. 1(a)). We initially screened 500 compounds to look for potential active candidates that inhibited ADAM10 activity by at least 50% at a concentration of 32 $\mu g \cdot mL^{-1}$ (Fig. S1(a) in Appendix A), and the most promising compound was kaempferol (Fig. 1(b)), a representative bioactive flavonol widely distributed in traditional Chinese herbs and dietary sources [25]. Consistently, a sub-cytolytic concentration of Hla induced a pronounced increase in ADAM10 metalloprotease activity, yet kaempferol dose-dependently reversed the rapid upregulation of ADAM10 activity triggered by Hla, and importantly, 4 $\mu g \cdot mL^{-1}$ kaempferol was sufficient to suppress ADAM10 activity to the baseline (Fig. 1(c)). Notably, the dose-dependent inhibition of kaempferol under native ADAM10 activity without Hla stimulation was also observed (Fig. S1(b) in Appendix A). Further investigations demonstrated that kaempferol did not exert a visible influence on the transcription (Fig. S1(c) in Appendix A) or expression (Fig. S1(d) in Appendix A) of ADAM10 in the host cells. To explore the potential mechanism by which kaempferol inhibits ADAM10 activity, a molecular docking study was performed to investigate the binding mode between them. Interestingly, kaempferol engaged in the zinc-dependent metalloprotease domain of ADAM10 primarily by interacting with the residues leucine 328 (Leu328), glycine 329 (Gly329), and threonine 380 (Thr380); and the active catalysis sites Histidine 383 and glutamic acid 384 (Glu384) (Fig. S1(e) in Appendix A), indicating that kaempferol may inactivate ADAM10 through direct binding.

Hla-caused activation of ADAM10 and the resulting proteolysis of cadherins, which plays a key role in maintaining barrier integrity, is the prominent mechanism of *S. aureus* dissemination [26]. It is therefore likely that kaempferol hinders Hla/ADAM10-mediated barrier disruption by inhibiting ADAM10 activity. To confirm this hypothesis, we first evaluated the effect of kaempferol

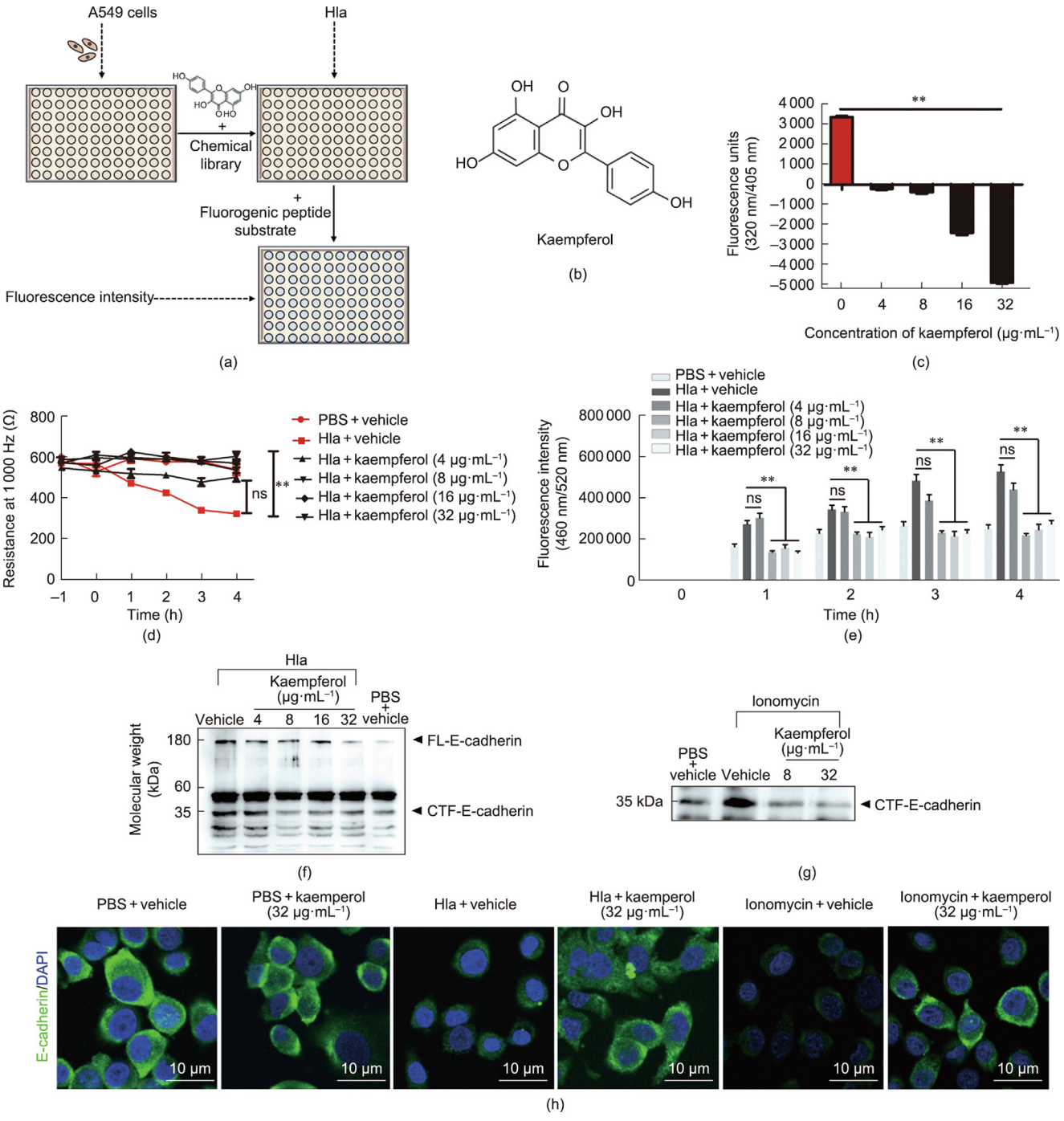

Fig. 1. Kaempferol prevents Hla-mediated barrier disruption as a potent ADAM10 inhibitor. (a) Diagram for compound screening of ADAM10 inhibitors. (b) Chemical structure of kaempferol. (c) Dose-dependent inhibition by kaempferol of cellular-based metalloprotease activity in A549 cells. The fluorescence intensity was measured on a Tecan Microplate Reader with excitation at 320 nm and emission at 405 nm. (d) TEER of A549 monolayers exposed to PBS or 50 μg·mL^{-1} Hla, supplemented with or without pretreatment using the indicated concentrations of kaempferol. (e) The permeability of the A549 monolayer to fluorescein following stimulation with PBS or 50 μg·mL^{-1} Hla, with or without kaempferol treatment. The percolated fluorescence was measured with excitation at 460 nm and emission at 520 nm. (f) Immunoprecipitation and immunoblot analysis of full-length (FL) and C-terminal fragment (CTF) of E-cadherin in A549 cells that were pretreated with the indicated concentrations of kaempferol for 3 h and then stimulated with 50 μg·mL^{-1} Hla or PBS for 1 h. (g) Immunoprecipitation and immunoblot analysis of FL and intracellular CTF of E-cadherin in A549 cells that were pretreated with the indicated concentrations of kaempferol for 3 h and then stimulated with 5 μmol·L^{-1} ionomycin or PBS for 1 h. (h) Immunofluorescence microscopy analysis of surface E-cadherin in A549 cells with indicated treatments. The nuclei were stained with DAPI (blue), and E-cadherin was stained with Alexa Fluor® 488 (green). Data are presented as the mean ± SEM (n = 3). Comparisons among multiple groups were performed by one-way ANOVA. **: P < 0.01 compared to the vehicle-treated group; ns: not significant.

on barrier function *in vitro* by measuring the TEER and permeability of the A549 epithelial monolayer exposed to Hla. Compared to PBS treatment, the addition of Hla at a concentration insufficient to cause cytotoxicity led to a rapid loss of resistance of A549 monolayer (Fig. 1(d)), which was accompanied by a significant increase in monolayer permeability (Fig. 1(e)), suggesting a remarkable injury to barrier integrity. As expected, kaempferol treatment reversed Hla-induced barrier dysfunction in a dose-dependent

manner and achieved significance at a concentration of 8 μg·mL^{-1}. These data demonstrated that kaempferol could effectively suppress Hla/ADAM10-mediated barrier disruption.

The TEER drop in the A549 monolayer is a direct outcome of increased proteolysis cleavage of E-cadherin by ADAM10, a process leading to the release of the extracellular N-terminal domain from E-cadherin and the appearance of an approximately 35-kDa intracellular C-terminal fragment (CTF) [27]. To clarify whether kaempferol abrogated Hla-mediated barrier disruption by blocking E-cadherin cleavage related to unusual ADAM10 activation, lysates from A549 cells with the indicated treatment were analyzed by immunoprecipitation and immunoblotting. Consistent with the TEER analysis, 50 μg·mL^{-1} Hla triggered the obvious cleavage of E-cadherin (Fig. 1(f)), and as expected, kaempferol completely blocked Hla-triggered E-cadherin cleavage at a concentration required to maintain barrier integrity (8 μg·mL^{-1}). Notably, treatment with 8 μg·mL^{-1} kaempferol also attenuated E-cadherin cleavage triggered by ionomycin (Fig. 1(g)), a calcium ionophore that enhances the cleavage of E-cadherin as an enzyme activator of ADAM10 [20]. Immunofluorescence microscopy analysis further revealed similar surface E-cadherin in the samples with kaempferol or PBS and the visible loss of surface E-cadherin in the samples upon Hla stimulation and ionomycin induction (Fig. 1(h)). As predicted, an attenuation of this loss was observed in cells treated with kaempferol. Taken together, our results demonstrated that kaempferol was a potent ADAM10 inhibitor that effectively prevented Hla-induced barrier disruption by suppressing the rapid upregulation of ADAM10 metalloprotease activity.

3.2. Kaempferol prevented Hla-caused barrier disruption in vivo

To investigate the *in vivo* effect of kaempferol on Hla-induced endothelial barrier disruption, a Miles assay was performed. As shown in Figs. 2(a) and (b), the subcutaneous injection of PBS did not cause obvious dye infiltration. By contrast, visible accumulation of the nonvascular permeable dye was observed in the area surrounding the Hla injection site in vehicle-treated mice, in which the endothelial integrity was breached, with obvious erythema and induration in the central region (Figs. 2(a) and (b)). Similar to the *in vitro* protection role in the epithelial barrier, kaempferol treatment also prevented endothelial barrier disruption by Hla in mice, as manifested by limited dye infiltration and gloss pathogenicity changes compared to the vehicle group (Figs. 2(a) and (b)). In addition, Hla challenge caused representative skin histological lesions in vehicle-treated mice, with a severely destroyed mastoid structure, a reduced number of sebaceous gland ducts, significantly disintegrated muscle fibers with visible necrosis, dissolved nuclei, and particularly, a loss of the granular layer under a microscope (Fig. 2(c)). Nonetheless, kaempferol treatment markedly alleviated this injury (Fig. 2(c)). Together, these results indicated that kaempferol could effectively hinder Hla-induced barrier disruption and tissue damage *in vivo*.

3.3. ADAM10 was involved in S. aureus-induced necroptosis

In addition to breaching the barrier integrity via ADAM10 interaction, Hla also enables *S. aureus* to break through the host immune system by inducing necroptosis, a newly identified pathogenic mechanism of *S. aureus* pneumonia [28]. A previous study showed that the ADAM10-mediated ectodomain shedding of cell-surface proteins could accelerate necroptosis downstream of TNF receptor 1 (TNFR1) and trigger a necroptosis-associated inflammatory response [12]. Given the rapid upregulation of ADAM10 by Hla, we asked whether ADAM10 was also required for *S. aureus*-mediated necroptosis, which is still unknown. To investigate this possibility, differentiated THP-1 cells were used in the current study. Consistently, challenges with wt *S. aureus* markedly increased the phosphorylation of RIP1/RIP3/MLKL (P-RIP1/P-RIP3, P-MLKL) mediators and caused significant cytotoxicity in cells transfected with irrelevant siRNA, while gene silencing using siRNA targeting *ADAM10* almost completely blunted these observations (Figs. 3(a)–(c)). Notably, *Δhla S. aureus* induced only a slight activation of the necroptosis pathway and significantly reduced cytotoxicity in both control cells and ADAM10-knockdown cells (Figs. 3(b) and (c)), which confirmed the indispensable role of both ADMA10 and Hla in *S. aureus*-induced necroptosis.

Apart from the phosphorylation of RIP1/RIP3/MLKL, the membrane translocation of MLKL is another critical hallmark of necroptosis, followed by the formation of clusters and hotspots (pore-like structures) on cell membranes and consequently of necrotic cell death [29]. Thus, we examined the localization of MLKL by immunofluorescence microscopy analysis. Consistent with the pathway analysis, the apparent translocation of MLKL was observed in THP-1 cells transfected with irrelevant siRNA and infected with wt *S. aureus* but not *Δhla S. aureus*, along with the obvious aggregation of MLKL at the plasma membrane and typical pore-like structures (Fig. 3(d)). By contrast, MLKL translocation was not observed in siADAM10-transfected cells (Fig. 3(d)). Collectively, these results demonstrated the indispensable role of Hla/ADAM10 in *S. aureus*-induced necroptosis for the first time and uncovered ADAM10 as a new potential host target for *S. aureus* infection based on necroptosis inhibition.

3.4. Kaempferol suppressed S. aureus-induced necroptosis via ADAM10 inhibition

Based on the above findings, we next verified whether kaempferol could block *S. aureus*-caused necroptosis through inhibiting ADAM10. As shown in Fig. 4(a), challenges with wt *S. aureus* led to the obvious phosphorylation of RIP1/RIP3/MLKL in THP-1 cells, consequently leading to high cytotoxicity (Fig. 4(b)). As speculated, kaempferol treatment (32 μg·mL^{-1}) almost blunted the activation of the necroptosis pathway triggered by wt *S. aureus* (Fig. 4(a)) as well as cell death (Fig. 4(b)). Intriguingly, although kaempferol did not exert an inhibitory effect on the minimal cytotoxicity conferred by *Δhla S. aureus* (Fig. 4(b)), the slight phosphorylation of MLKL induced by *Δhla S. aureus* was abrogated by adding kaempferol (Fig. 4(a)), indicating a potential role for kaempferol in the pathway irrelevant to Hla. MLKL pore formation could also reportedly activate the inflammasomes, therefore boosting the production of IL-1β [30]. Thus, we further measured IL-1β production in cells infected with *S. aureus*. Consistent with the analysis of MLKL activation, the IL-1β production elicited by both wt *S. aureus* and *Δhla S. aureus* was significantly suppressed in the presence of kaempferol (Fig. 4(c)).

To verify the effect of kaempferol on this mode of programmed cell death, the cells were stained with live/dead reagent containing both membrane-impermeable (red) and membrane-permeable (green) fluorescent dyes. Consistent with the results of the LDH release assay, a considerable proportion of cells infected with wt *S. aureus* were stained with membrane-impermeable red fluorescent dye, indicating perforation of the cell membrane by MLKL pore formation (Fig. 4(d) and Fig. S2(a) in Appendix A). By contrast, the percentage of dead cells with red fluorescence was significantly reduced by kaempferol treatment (32 μg·mL^{-1}). Conversely, most cells without bacterial stimulation or those infected with *Δhla S. aureus* were stained with membrane-permeable green fluorescent dye. Furthermore, kaempferol treatment exerted no toxicity on the cells, given that almost no red fluorescence was observed in the uninfected or *Δhla S. aureus*-infected samples. Based on the above

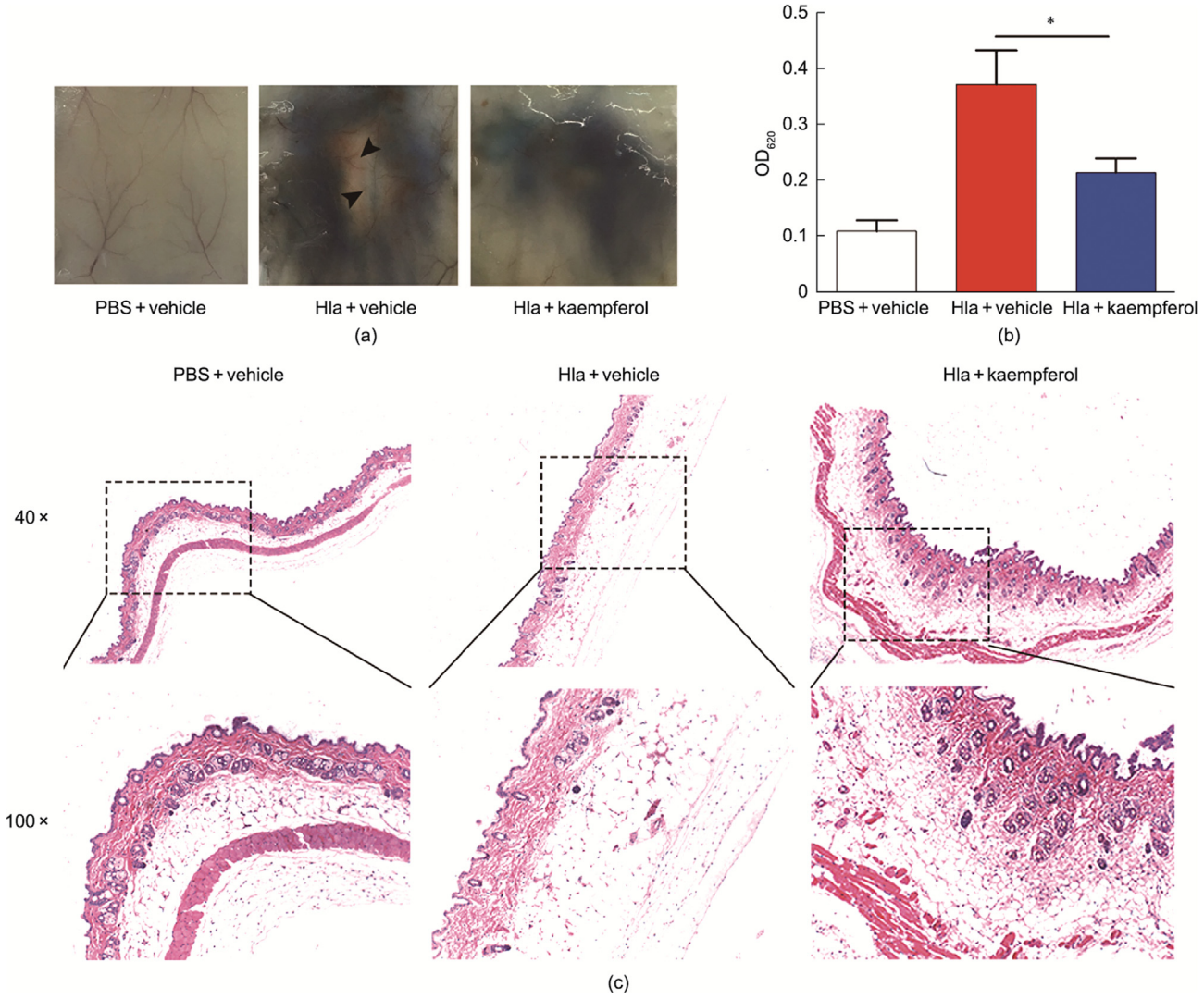

Fig. 2. Kaempferol is protective against Hla-induced endothelial barrier disruption and subsequent skin injury in mice. (a) Visible accumulation of Evans blue dye surrounding the PBS or Hla injection site. BALB/c mice were subcutaneously injected with vehicle or a single dose of 100 mg·kg^{-1} kaempferol 8 h prior to the experiment and then subcutaneously injected with 7.5 μg of Hla in 100 μL of PBS or an equal volume of PBS for the Miles assay. n = 5 mice per group. Arrows indicate the gross lesions in the skin. (b) Quantification of Evans blue dye extravasation from the vasculature into the skin. The Evans blue dye in the skin was extracted by formamide at 65 °C for 24 h and spectrophotometrically detected at 620 nm. (c) Histopathological examination of skin tissues from mice pretreated with vehicle or kaempferol and subcutaneously injected with 7.5 μg of Hla in 100 μL of PBS or an equal volume of PBS. The data are presented as the mean ± SEM. The statistical significance between two independent groups was determined by unpaired two-tailed Student's t test. *: P < 0.05 compared to the vehicle-treated group.

results, we further examined the effect of kaempferol on the membrane translocation of MLKL. As shown in Fig. 4(e), challenges with wt *S. aureus*, but not *Δhla S. aureus*, resulted in the obvious aggregation of MLKL at the plasma membrane, which was also suppressed by kaempferol treatment (Fig. S2(b) in Appendix A). Promisingly, the dose-dependent inhibition of kaempferol on wt *S. aureus*-induced cytotoxicity was observed in THP-1 cells (Fig. S2(c) in Appendix A) and other host cells, including MPMs (Fig. S2(d) in Appendix A) and A549 cells (Fig. S2(e) in Appendix A).

Then, we further determined whether necroptosis inhibition by kaempferol relied on ADAM10. Consistent with our hypothesis, kaempferol treatment significantly inhibited wt *S. aureus*-induced necroptosis and cytotoxicity in the control cells (Figs. 4(f) and (g)). However, an *ADAM10* knockdown using siRNA eliminated necroptosis activation by wt *S. aureus* infection as well as the inhibitory effect of kaempferol. Interestingly, the wt *S. aureus*-induced activation of the necroptosis pathway was also remarkably impaired by EDTA, a broad-spectrum inhibitor of metalloproteinase, indicating that both the expression and activity of ADAM10 were required for *S. aureus*-induced necroptosis. As gene silence did, EDTA treatment abrogated the inhibition of necroptosis by kaempferol (Fig. 4(h)), suggesting that kaempferol could effectively block *S. aureus*-induced necroptosis by inhibiting ADAM10 activity.

Additionally, we evaluated the potential antibacterial effect of kaempferol on *S. aureus*. Consistent with previous research [31], the MIC of kaempferol against *S. aureus* strains was greater than 1024 μg·mL^{-1}. Consistently, bacteria treated with the indicated concentrations of kaempferol exhibited similar growth trends compared with the control group (Figs. S3(a)–(c) in Appendix A). Importantly, we further analyzed the intracellular survival of *S. aureus* in differentiated THP-1 cells. Consistent with a previous study that ruled out the participation of Hla in the escape of *S. aureus* from human macrophages [18], *Hla* deficiency had no significant effect on the intracellular survival of *S. aureus* within THP-1 macrophages, and kaempferol treatment (32 μg·mL^{-1}) did not exhibit a visible impact on *S. aureus* intracellular infection in THP-1 cells (Fig. S3(d) in Appendix A).

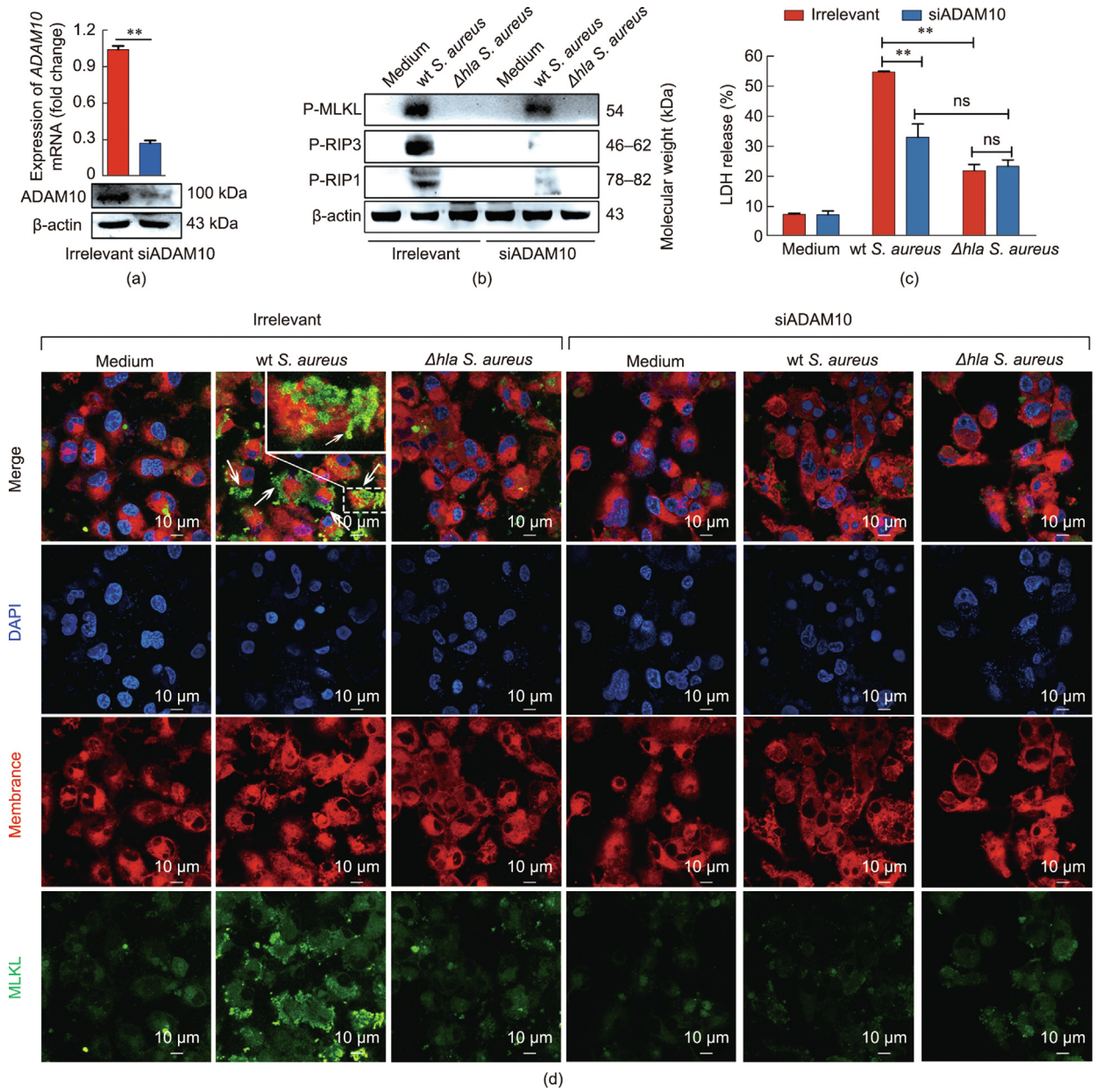

Fig. 3. ADAM10 is required for *S. aureus*-induced necroptosis. (a) Immunoblot analysis of ADAM10 in THP-1 cells transfected with irrelevant siRNA or siRNA targeting *ADAM10* (siADAM10). Forty-eight hours after transfection, the messenger RNA (mRNA) and protein levels were examined by qRT-PCR and immunoblot analysis, respectively. (b) Immunoblot detection of necroptosis mediators in THP-1 cells transfected with siRNA or siADAM10 following challenges with wt *S. aureus* or *Δhla S. aureus*. Transfected cells were infected with *S. aureus* at an MOI of 20 for 6 h. (c) Cytotoxicity of transfected THP-1 cells infected with wt *S. aureus* or *Δhla S. aureus* for 6 h at an MOI of 20. (d) Localization of MLKL (green) in THP-1 cells transfected with irrelevant siRNA or siADAM10 and then infected with wt *S. aureus* or *Δhla S. aureus* for 6 h at an MOI of 20. The lipid membranes (red) and nuclei (blue) were stained with DiD and DAPI, respectively. Arrows point to the typical clusters (pore-like structures) of MLKL on the membrane. The data are presented as the mean ± SEM (n = 3). The statistical significance between two independent groups was determined by unpaired two-tailed Student's t test. **: $P < 0.01$ compared to cells transfected with irrelevant siRNA.

Taken together, our results established that kaempferol prevented cells from Hla-mediated cytotoxicity through the ADAM10-dependent blockage of the necroptosis pathway, rather than the action against *S. aureus* viability or intracellular survival.

3.5. *Kaempferol suppressed* S. aureus*-induced necroptosis through interfering with the interplay between ADAM10 and TNF necroptosis signaling*

We next addressed the potential mechanism by which kaempferol inhibited necroptosis. Necroptosis can be induced by several exogenous or endogenous biological stimuli, such as the toll-like receptor (TLR) ligands LPS (TLR4) and poly(I:C) (TLR3) and TNF. In contrast to TNF-α, which activates RIP1 via TNFR1, LPS-induced RIP1 activation and necroptosis are dependent on Toll-interleukin-1 receptor domain-containing adapter-inducing interferon-beta (TRIF). Despite this characteristic, LPS-induced necroptosis follows the same pathway downstream of TNF death receptor activation [32]. Using L929 cells, we observed that TNF-induced necroptosis was attenuated by kaempferol in a dose-dependent manner, as manifested by reduced cytotoxicity and PI uptake (Figs. 5(a) and (b)). By contrast, kaempferol did not exert a similar suppressive effect on LPS-induced necroptosis in BMDMs in the absence of caspase activity (Figs. 5(c) and (d)).

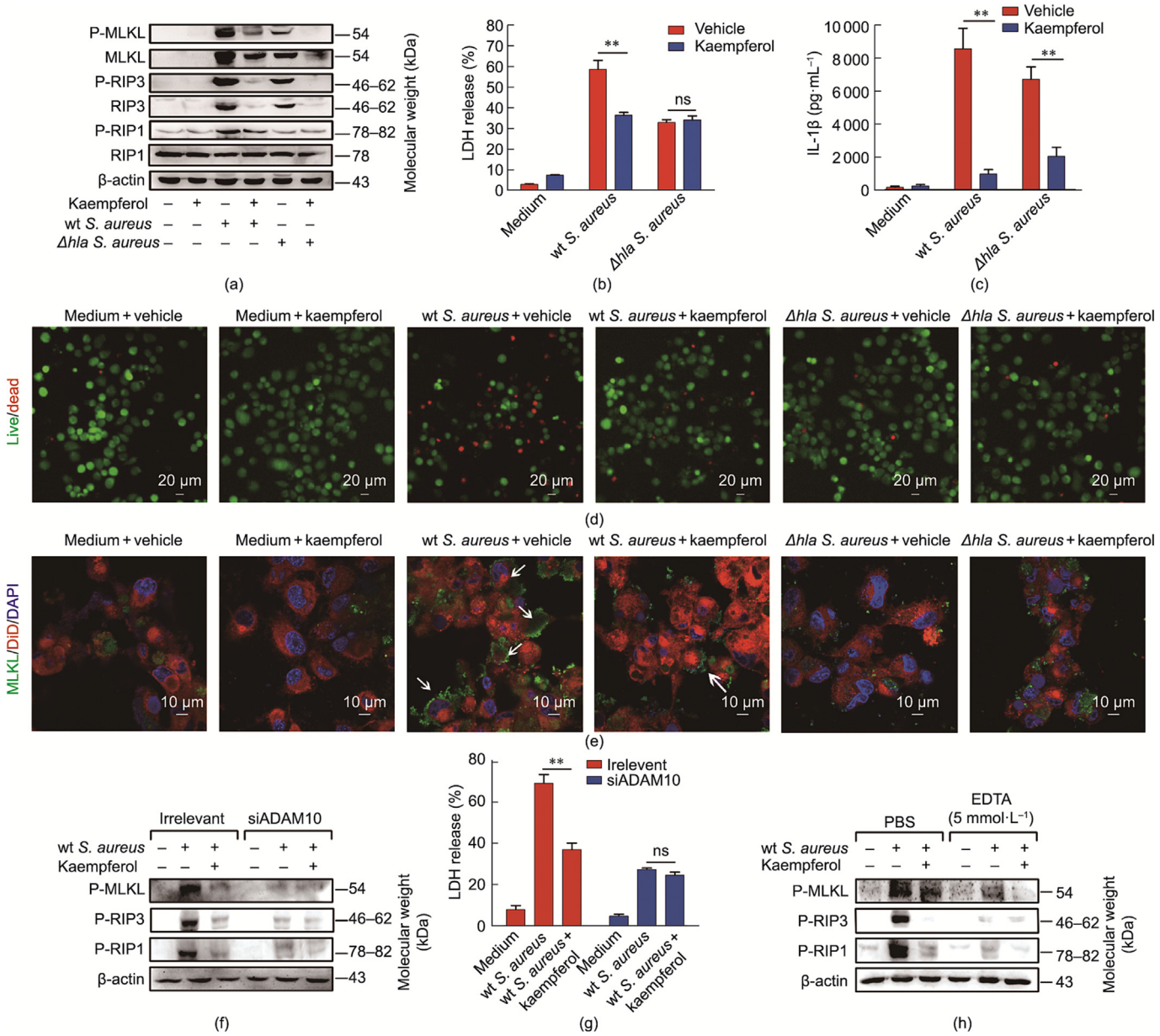

Fig. 4. Kaempferol suppresses *S. aureus*-caused necroptosis via ADAM10 inhibition. (a) Immunoblot analysis of the necroptosis cascade in THP-1 cells infected with wt *S. aureus* or *Δhla S. aureus* for 6 h (MOI = 20) in the presence of 32 μg·mL^{-1} kaempferol or vehicle. (b) The cytotoxicity of THP-1 cells with the above treatment was determined with a Cytotoxicity Detection Kit. (c) IL-1β levels in the supernatants of THP-1 cells with the above treatment were measured using ELISA, and (d) the cells in the bottom of the wells were stained with live (green)/dead (red) reagent. (e) Immunofluorescence for the localization of MLKL (green) in THP-1 cells with the above treatment for 6 h (MOI = 20). The lipid membrane (red) and nuclei (blue) were stained with DiD and DAPI, respectively. Arrows point to the typical clusters (pore-like structures) of MLKL on the membrane. (f) Effects of *ADAM10* silencing on kaempferol-driven necroptosis inhibition upon wt *S. aureus* infection. THP-1 cells transfected with siRNA or siADAM10 were infected with wt *S. aureus* for 6 h (MOI = 20) and pretreated with kaempferol (32 μg·mL^{-1}) or the vehicle for 3 h. (g) The cytotoxicity of THP-1 cells with the above treatment was determined using a Cytotoxicity Detection Kit. (h) Effects of EDTA, a broad-spectrum inhibitor of metalloproteinases, on kaempferol-driven necroptosis inhibition upon wt *S. aureus* infection. The data are presented as the mean ± SEM (n = 3). The statistical significance between two independent groups was determined by unpaired two-tailed Student's t test. **: P < 0.01 compared to the vehicle-treated group.

The differential effect of kaempferol on TNF-induced necroptosis and LPS-induced necroptosis excluded the possibility that kaempferol blocked necroptosis via direct inhibition of the mediators in the necroptosis pathway. Thus, kaempferol suppressed TNF-induced necroptosis by targeting ADAM10 because ADAM10 activation was required to accelerate necroptosis upon TNF-α stimulation [12]. Together, our results indicated that kaempferol suppressed *S. aureus*-induced necroptosis via blocking the interplay between ADAM10 metalloproteinase activity and TNF necroptosis signaling.

3.6. *Kaempferol reduced* S. aureus*-evoked inflammatory response via inhibition of ADAM10*

Necroptosis is known as highly proinflammatory lytic cell death because the pore formation of MLKL can directly cause membrane rupture with a massive leakage of danger-associated molecular patterns (DAMPs) to induce a strong inflammatory response and consequently boost proinflammatory genes [33]. Therefore, we also explored whether kaempferol could suppress *S. aureus*-evoked inflammatory response. As expected, the dramatic

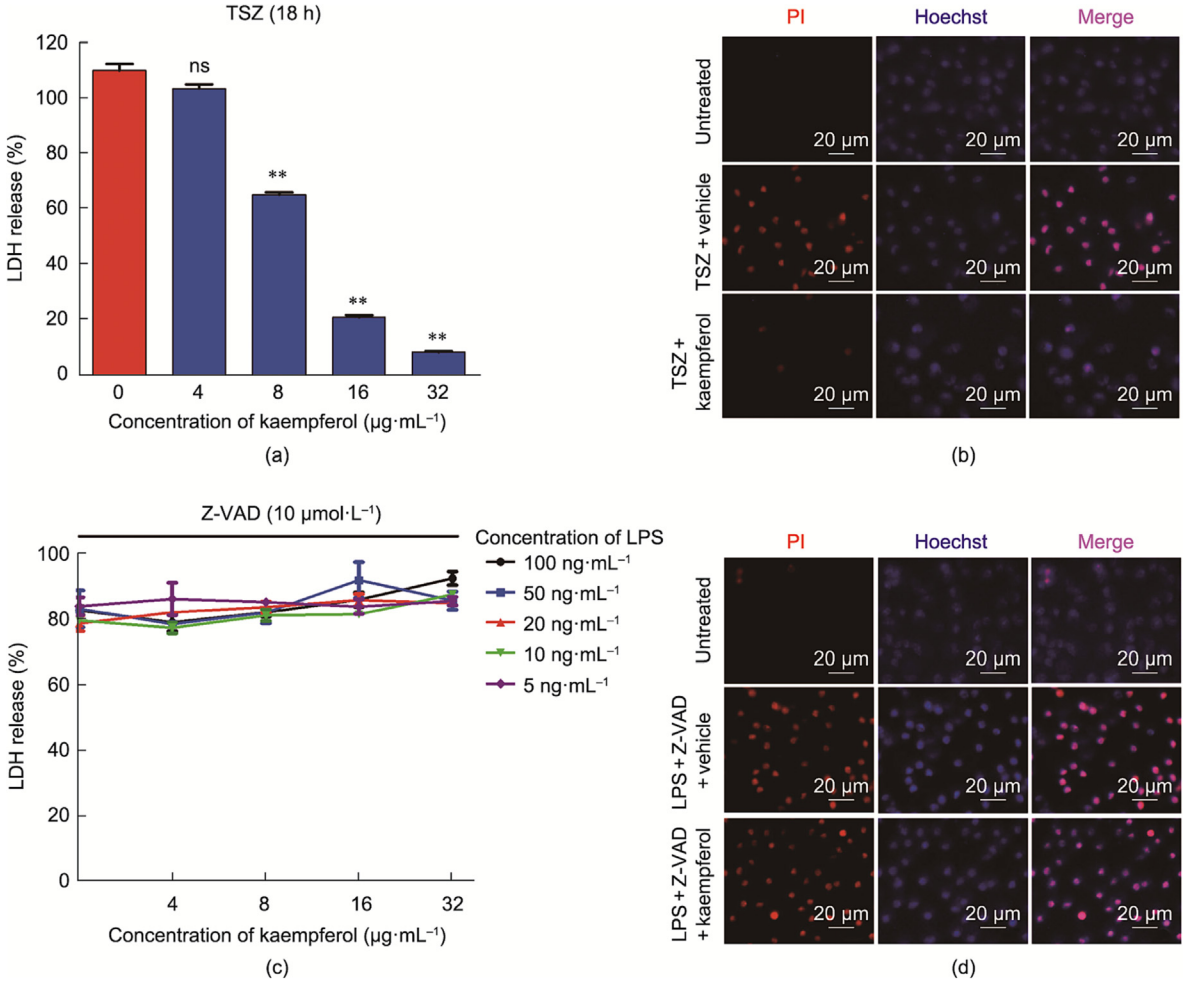

Fig. 5. Kaempferol suppresses TNF-induced necroptosis, but not LPS. (a) Cytotoxicity of L929 cells stimulated by TSZ for 18 h in the presence of the indicated concentrations of kaempferol. (b) The cell death of L929 cells visualized by PI and Hoechst staining. L929 cells were pretreated with 32 μg·mL^{-1} kaempferol or vehicle for 3 h and then stimulated with TSZ for 18 h. (c) Cytotoxicity of BMDMs induced by LPS in the absence of caspase activity for 24 h. BMDMs were pretreated with the indicated concentrations of kaempferol for 3 h and then stimulated with 10 μmol·L^{-1} Z-VAD and the indicated LPS concentrations for 24 h. (d) Cell death of BMDMs as visualized by PI and Hoechst staining. BMDMs were pretreated with 32 μg·mL^{-1} kaempferol or vehicle for 3 h and then stimulated with 10 μmol·L^{-1} Z-VAD and 10 ng·mL^{-1} LPS for 24 h. The data are presented as the mean ± SEM (n = 3). The statistical significance between multiple groups was determined by one-way ANOVA. **: P < 0.01 compared to the vehicle-treated group.

activation of the MAPK and NF-κB signaling pathways upon *S. aureus* stimulation was almost completely blocked by kaempferol treatment (Figs. 6(a) and (b)), with attenuated phosphorylation levels of inflammatory mediators, including p38, ERK, JNK, IKK, and p65. As a result, the transcription levels of the proinflammatory genes *IL-1β* (Fig. 6(c)), *TNF-α* (Fig. 6(d)), *IL-6* (Fig. 6(e)), and *CXCL1* (Fig. 6(f)) were all significantly reduced following kaempferol treatment. In fact, ADAM10 can also directly control these two signaling cascades in a manner dependent on its metalloproteinase activity [34,35]. Therefore, kaempferol-mediated inhibition of the inflammatory response and proinflammatory gene transcription was also observed in *Δhla S. aureus*-infected cells (Fig. 6). We then found that the activation of NF-κB and MAPK pathway in response to *S. aureus* infection was remarkably attenuated by *ADAM10* silencing using siRNA (Fig. S4 in Appendix A). Consistently, the extraordinary inhibitory effect of kaempferol was also impaired in *ADAM10*-knockdown cells (Fig. S4). Taken together, these data demonstrated that kaempferol effectively reduced *S. aureus*-evoked inflammation response through inhibiting ADAM10, which was potentially related to necroptosis inhibition as well as the direct contribution of ADAM10 to inflammation.

3.7. *Kaempferol was protective against* S. aureus *pneumonia and mastitis in mice*

Next, we investigated the *in vivo* effect of kaempferol on *S. aureus* pneumonia and a mastitis model. MRSA strain USA300 and methicillin-susceptible *Staphylococcus aureus* (MSSA) strain NTCC 8325-4, which represented the methicillin-resistant clinical strain and standard laboratory strain, respectively, were used to establish lethal pneumonia infections. As expected, pretreatment with kaempferol (100 mg·kg^{-1}) for 8 h before *S. aureus* challenge effectively protected mice from lethal *S. aureus* pneumonia. The survival rate of mice challenged with 6×10^8 CFUs of NTCC 8325-4 was significantly enhanced by kaempferol treatment (P = 0.0488), with an increase of 38.46% (Fig. 7(a)). In the mice challenged with 2×10^8 CFUs USA300, the survival rate was increased from 38.46% to 84.62%, with an increase of 46.16% (P = 0.0119) (Fig. 7(b)). To better mimic the clinical situation in which pneumonia often occurs only after the infection has already been established, kaempferol administration was deferred until just after MRSA USA300 challenge. Promisingly, kaempferol significantly delayed death and increased the survival rate by 33.33% when administered following

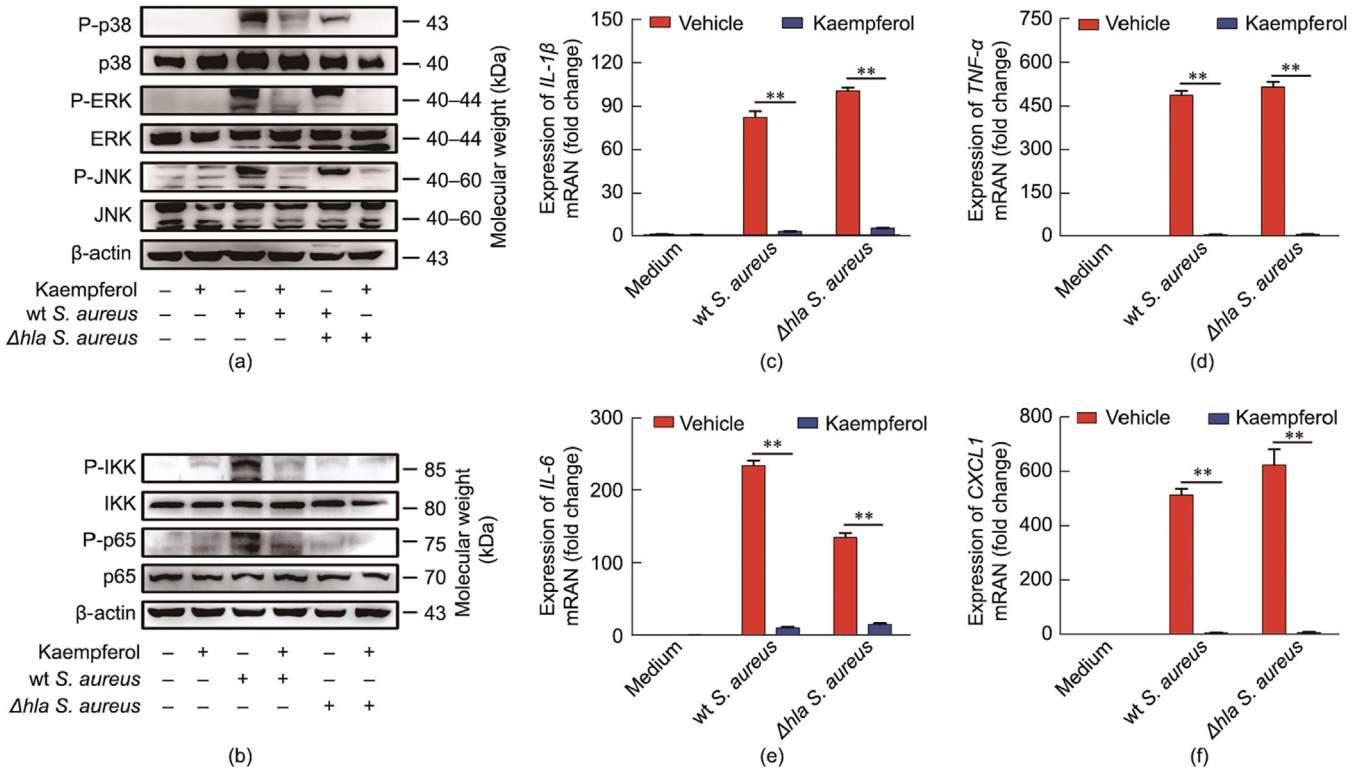

Fig. 6. Kaempferol inhibits *S. aureus*-evoked inflammatory response. Effect of kaempferol on the activation of (a) MAKP signaling pathway and (b) NF-κB signaling pathway evoked by *S. aureus* infection. THP-1 cells were pretreated with 32 $\mu g \cdot mL^{-1}$ kaempferol or vehicle for 3 h, followed by an infection with wt *S. aureus* or *Δhla S. aureus* at an MOI of 10 for 6 h. Whole cell lysates were probed with specific antibodies against the indicated inflammatory mediators. The levels of phospho-p38, -ERK, -JNK, -p65, and -IKK (P-p38, P-ERK, P-JNK, P-p65, and P-IKK) relative to β-actin were determined by densitometry. The mRNA levels of (c) IL-1β, (d) TNF-α, (e) IL-6, and (f) CXCL1 were quantified by qRT-PCR and normalized to GAPDH. The data are presented as the mean ± SEM (n = 3). The statistical significance between two independent groups was determined by unpaired two-tailed Student's t test. **: $P < 0.01$ compared to the vehicle-treated group.

S. aureus infection (Fig. S5 in Appendix A), confirming that kaempferol was effective as a treatment.

Sublethal infection with USA300 caused dark red lesions with extravasated blood in the lungs derived from mice that received vehicle treatment (Fig. 7(c)), and histopathological examination revealed severe edema with visible swelling and congestion. Conversely, both gross and histopathologic lesions were greatly alleviated in the infected mice treated with kaempferol (Fig. 7(c)). Additionally, kaempferol treatment also markedly decreased the bacterial load (Fig. 7(d)), wet/dry weight ratio (Fig. 7(e)), and MPO activity (Fig. 7(f)) in the lung tissues of infected mice. Acute lung injury caused by *S. aureus* infection is often accompanied by the loss of alveolar barrier function and the excessive secretion of cytokines. Consistent with the Miles assay results, kaempferol administration effectively preserved the integrity of the alveolar barrier, which was evidenced by significantly reduced cell infiltration and protein leakage in the BALF (Figs. 7(g) and (h)). Furthermore, the levels of IL-1β, TNF-α and IL-6 in the BALF were also strongly reduced (Fig. 7(i)). In conclusion, these results demonstrated that kaempferol treatment provided effective protection against *S. aureus* pneumonia.

For *S. aureus* mastitis infection, the histopathology examination revealed that kaempferol treatment visibly reduced mammary gland injury and inflammatory cell infiltration caused by *S. aureus* (Fig. 8(a)). In addition, the bacterial loads in mice mammary gland tissues derived from kaempferol-treated mice were much lower than those from mice that received vehicle ($P < 0.01$) (Fig. 8(b)). Moreover, the production of proinflammatory cytokines in the mammary gland tissues of infected mice was also significantly reduced following kaempferol treatment (Figs. 8(c)–(e)). Taken together, our results established that kaempferol is a potential treatment against *S. aureus* infection, such as pneumonia and mastitis, in mice.

4. Discussion

The key role of Hla in *S. aureus* pathogenicity renders it as a promising therapeutic target based on an anti-virulence strategy. Several inhibitors and antibodies targeting Hla have been reported in the past few years [36]. However, a host-directed antibacterial strategy of targeting Hla's specific cellular receptor ADAM10 has not been characterized. ADAM10 stands out for its indispensable role in mediating Hla pore formation in *S. aureus* pathogenesis. Dramatically, Hla pore formation in turn leads to the Ca^{2+}-dependent activation of ADAM10 metalloproteinase activity, resulting in severe barrier disruption by cleaving cell surface adhesins and initiating the intracellular signaling events that contribute to the dissolution of focal adhesions, which facilitates bacterial spreading and maximally determines the outcome of *S. aureus* infections [37]. As such, the inhibition of ADAM10 activity or interfering with the formation of Hla/ADAM10 complex is a developable strategy to curb *S. aureus* infection. In addition to causing cadherin disruption in barrier-forming cells and therefore accelerating invasive infection through upregulating ADAM10, Hla also triggers RIP1/RIP3/MLKL-mediated necroptosis, a newly identified mechanism of *S. aureus* infection representing another novel target for drug design [38].

Our striking observation was that ADAM10 was also involved in *S. aureus*-mediated necroptosis. Although the role and mechanism of ADAM10 and necroptosis in *S. aureus* pathogenesis as well as the interplay between ADAM10- and TNF-induced necroptosis has

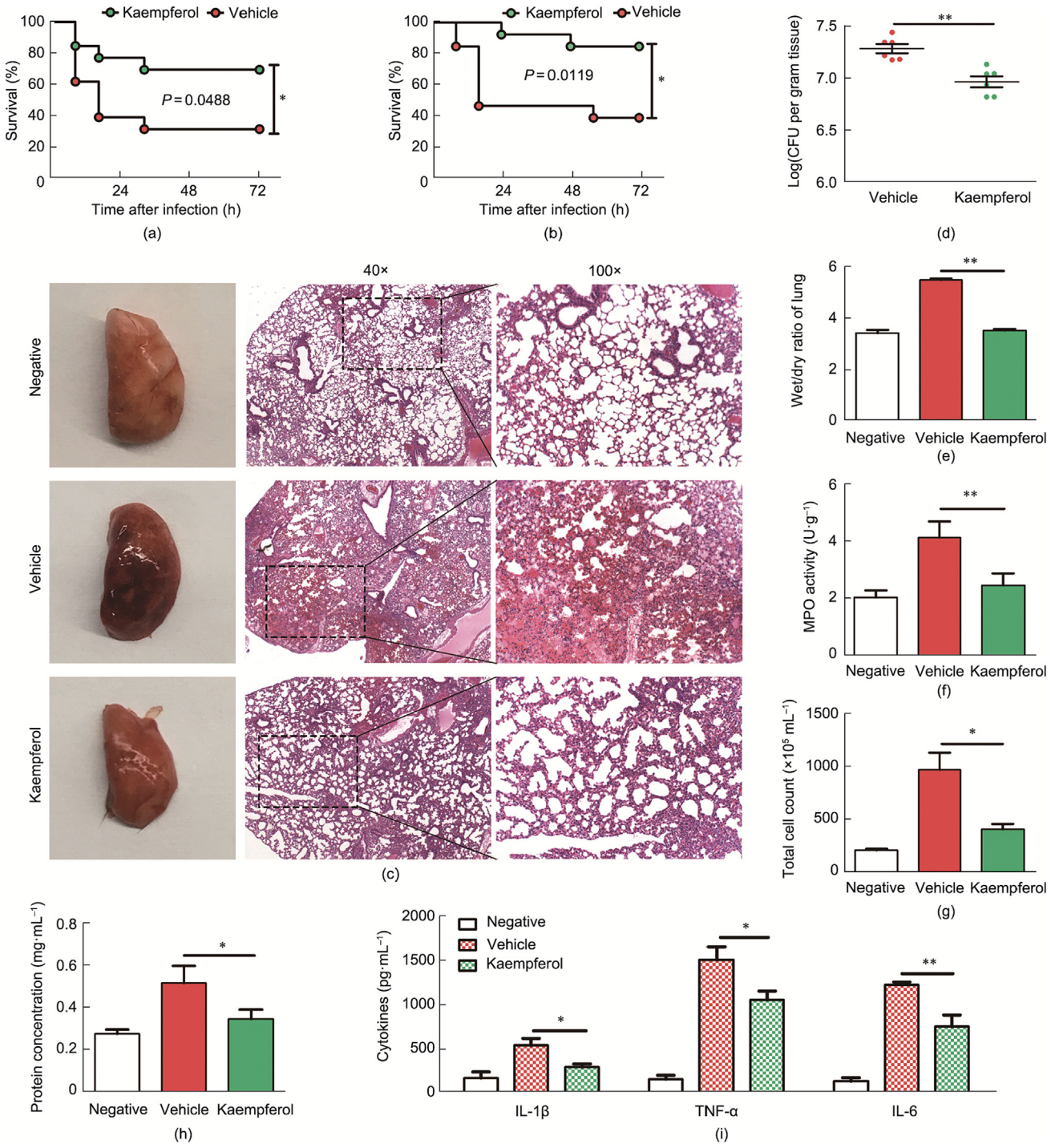

Fig. 7. Kaempferol protects mice from lethal *S. aureus* pneumonia. (a) Mortality of wt *S. aureus* NTCC 8325-4-infected female C57BL/6 mice. n = 13 mice per group. (b) Mortality of MRSA USA300-infected mice. n = 13 mice per group. (c) Gross pathology and histopathology of murine lungs (left) at 24 h post-infection. (d) The remaining lung tissues were homogenized in PBS (10% w/v) to analyze the bacterial burden by microbiological plating. n = 6 mice each group. (e) Wet/dry weight ratio of murine lungs. n = 6 mice per group. Additionally, (f) the remaining lung tissues were used to assess the MPO activity using an MPO detection kit. (g) A BAL assay for assessing cell infiltration and (h) protein exudation was performed to evaluate alveolar barrier disruption. n = 6 mice per group. (i) The cytokine concentrations in the BALF were measured using an ELISA. The mouse survival rate was analyzed using the log-rank (Mantel-Cox) test. The data are presented as the mean ± SEM. The statistical significance between two independent groups was determined by unpaired two-tailed Student's t test. *: $P < 0.05$, **: $P < 0.01$ compared to the vehicle-treated group.

been extensively investigated in recent years, the potential participation of ADAM10 in *S. aureus*-mediated necroptosis remains unclear. In the present study, we were the first to find that ADAM10 is required for *S. aureus* to activate the necroptosis pathway, as evidenced by the silencing of *ADAM10*, eliminating the activation of necroptosis and cytotoxicity upon *S. aureus* stimulation. These findings enhance our knowledge of ADAM10 in *S. aureus* infection, uncovering a new contribution of ADAM10 to *S. aureus*-induced necroptosis.

More importantly, we have successfully identified kaempferol, a natural small molecule, as an effective inhibitor of the enzymatic activity of ADAM10 without affecting ADAM10 expression and

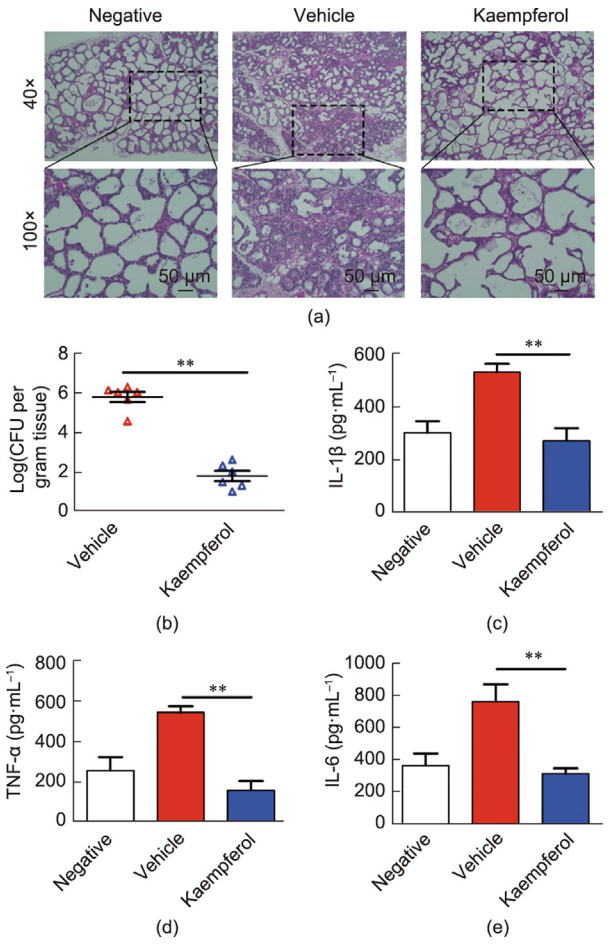

Fig. 8. Kaempferol confers effective protection against *S. aureus*-induced mastitis in mice. Lactating BALB/c mice were used to establish *S. aureus* mastitis through the intraductal inoculation of 5×10^6 CFUs USA300 bacteria. The mice were pretreated with kaempferol (100 mg·kg^{-1}) or vehicle by subcutaneous injection for 8 h before bacterial inoculation, and drug administration was maintained at an interval of 8 h after infection. Murine mammary gland tissues were harvested at 24 h post-infection. n = 6 mice per group. (a) Histopathologic examination by H&E staining of mammary gland tissues derived from each mouse that received the indicated treatment. (b) Bacterial burden in mammary gland tissues as determined by microbiological plating. The levels of (c) IL-1β, (d) TNF-α, and (e) IL-6 in the 10% tissue homogenates (w/v) were assessed by ELISA. The data are presented as the mean ± SEM. The statistical significance between two independent groups was determined by unpaired two-tailed Student's t test. **: $P < 0.01$ compared to the vehicle-treated group.

activation processes. In the present study, the molecular docking experiment revealed that kaempferol potentially inhibited ADAM10 activity by directly interacting with the residues Leu328, Gly329, and Thr380 and especially the active catalysis sites Hid383 and Glu384 in the zinc-dependent metalloprotease domain. Our data indicated that kaempferol could efficiently restrain Hla-induced barrier disruption by suppressing ADAM10-mediated cleavage of cadherins (Fig. 9). In this way, kaempferol might also function against other bacterial infections because, except for Hla, several PFTs derived from both Gram-negative and -positive bacteria share the ability to cause Ca^{2+} influx and the subsequent ADAM10 activation and cadherin cleavage, including *Streptococcus pneumoniae* pneumolysin [6], *Pseudomonas aeruginosa* ExlA, and *Serratia marcescens* ShlA [39]. Somewhat surprisingly, by functioning as an inhibitor of ADAM10 enzymatic activity rather than a signaling component of the necroptosis cascade, kaempferol also exhibited a significant suppressive effect on *S. aureus*-induced necroptosis and the inflammatory response, which might be associated with the interplay between ADAM10 metalloproteinase activity and TNF necroptosis signaling (Fig. 9). It is worth noting that necroptosis is also a common consequence of PFTs. In addition to *S. aureus*, several PFT-producing pathogens, including *Streptococcus pneumoniae*, *Serratia marcescens*, *Listeria monocytogenes*, and uropathogenic *Escherichia coli* [40], could all trigger necroptosis depending on the pore formation of those cytotoxins. The findings in our study have indicated that ADAM10 activation might also be involved in the necroptosis triggered by these pathogens. Additionally, our findings further shed light on the potential therapeutics power of kaempferol for treating PFT-producing bacteria due to its inhibition on ADAM10 activity and ADAM10-modulated necroptosis.

In vivo, kaempferol treatment conferred effective protection against MRSA and MSSA infection, confirming that ADAM10 inhibition is a viable strategy for curbing *S. aureus* infection. With the declining effectiveness of broad-spectrum antibiotics and the increasing cases of resistant *S. aureus* infections, the combination of ADAM10 inhibitors, including kaempferol and antibiotics, may greatly improve the clinical outcome by simultaneously acting directly against the pathogen and the host target that accelerate bacterial pathogenesis. In addition, ADAM10 has been implicated as a promising therapeutic target for multiple pathological processes in other diseases, ranging from breast cancer and chronic liver inflammation to Huntington's disease [41]. Our findings suggest the possibility of developing kaempferol as a drug candidate for diseases associated with ADAM10 upregulation. The most recent research reported that kaempferol prevents dopaminergic neuronal degeneration in Parkinson's disease and other neurodegenerative disorders (NDs) by promoting autophagy [14,42]. Here, we emphasized that the inhibitory effect of kaempferol on ADAM10 should be carefully considered when applying kaempferol to ND treatment because the upregulation of ADAM10 is in fact beneficial to NDs by promoting the clearance of amyloid deposits [43].

In conclusion, this study is the first to provide insights into the contribution of ADAM10 to *S. aureus*-induced necroptosis, which enhances our knowledge of ADAM10 in *S. aureus* infection. More importantly, we also identified kaempferol as a novel ADAM10 inhibitor that effectively eliminated the Hla-induced rapid upregulation of ADAM10 activity and thereby abrogated the consequent barrier disruption and necroptosis during *S. aureus* infection, which paved the way for the development of therapeutic strategy for diseases dependent on ADAM10 upregulation. In view of the broad participation of ADAM10 in both infectious and noninfectious diseases, kaempferol-driven ADAM10 inhibition may have important implications for drug development.

Acknowledgments

This work was supported by the National Natural Science Foundation of China (U22A20523, 32172912, and 32102722) and the Interdisciplinary Integration and Innovation Project of Jilin University (JLUXKJC2021QZ04).

Authors' contribution

Xuming Deng and Qianghua Lv designed the study, conceived and supervised the experiments, and reviewed and edited the manuscript. Tingting Wang and Jianfeng Wang performed most of the experiments and wrote the manuscript with the input from all the authors. Xiangzhu Xu, Fan Jiang, Hongfa Lv, Qinghui Qi, and Can Zhang performed some of the experiments and analyzed the data. Jianfeng Wang analyzed the data and reviewed the manuscript.

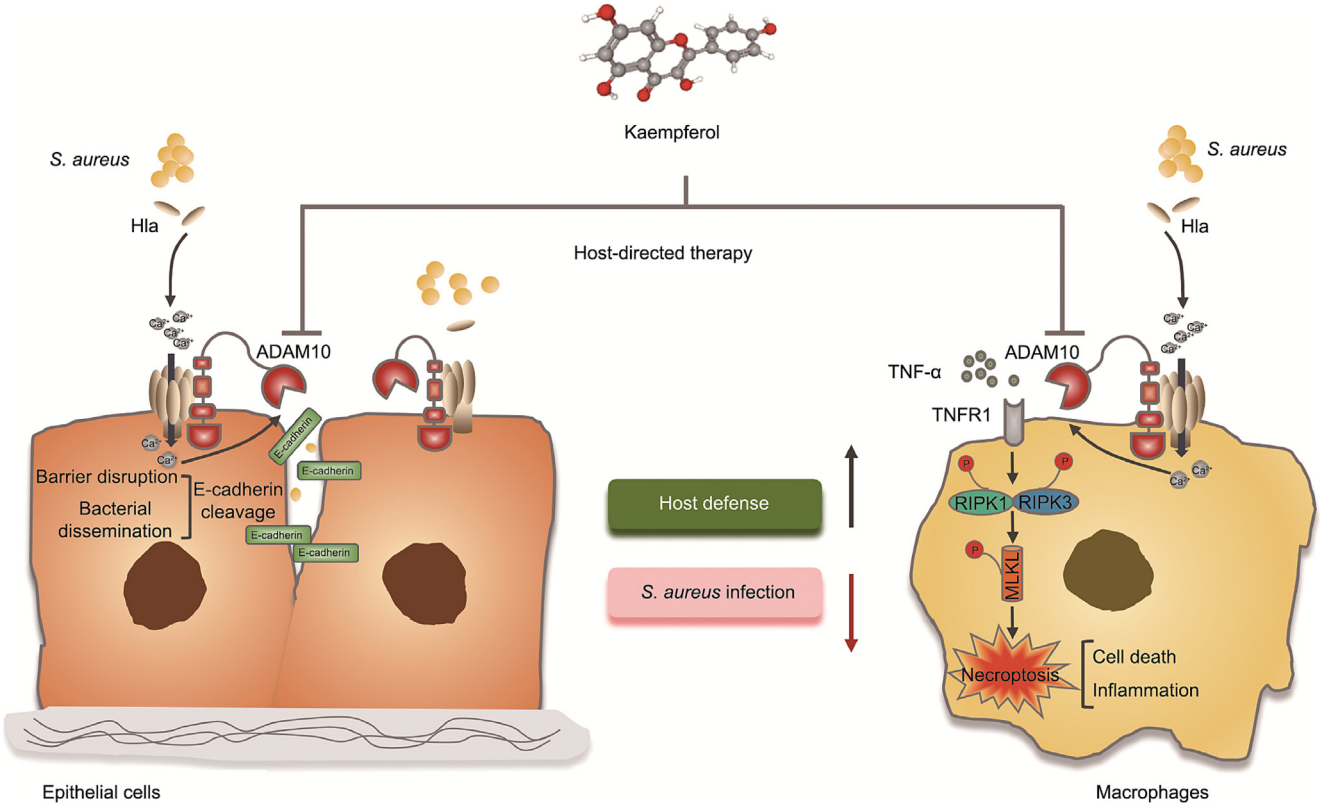

Fig. 9. Schematic model of HDT against *S. aureus* infection by kaempferol. HDT is an emerging alternative approach for treating infectious diseases, and ADAM10 represents a promising therapeutic target to curb *S. aureus* infection based on HDT. In this study, we identified the small molecule compound kaempferol as an effective ADAM10 inhibitor that abrogates Hla-induced rapid upregulation of ADAM10 and thereby restricts the epithelial barrier disruption and bacterial dissemination resulting from the cleavage of E-cadherin by ADAM10. Meanwhile, kaempferol also significantly blocked *S. aureus*-induced necroptosis and inflammation in macrophages through interfering with the interplay between ADAM10 metalloproteinase activity and TNF necroptosis signaling.

Compliance with ethics guidelines

Tingting Wang, Jianfeng Wang, Xiangzhu Xu, Fan Jiang, Hongfa Lv, Qinghui Qi, Can Zhang, Qianghua Lv, and Xuming Deng declare that they have no conflict of interest or financial conflicts to disclose.

Appendix A. Supplementary data

Supplementary data to this article can be found online at https://doi.org/10.1016/j.eng.2023.03.006.

References

[1] Schwegmann A, Brombacher F. Host-directed drug targeting of factors hijacked by pathogens. Sci Signal 2008;1(29):re8.
[2] Huang D, Luo JJ, OuYang X, Song L. Subversion of host cell signaling: the arsenal of rickettsial species. Front Cell Infect Mi 2022;12:995933.
[3] Seilie ES, Bubeck WJ. *Staphylococcus aureus* pore-forming toxins: the interface of pathogen and host complexity. Semin Cell Dev Biol 2017;72:101–16.
[4] Wilke GA, Bubeck WJ. Role of a disintegrin and metalloprotease 10 in *Staphylococcus aureus* alpha-hemolysin-mediated cellular injury. Proc Natl Acad Sci USA 2010;107(30):13473–8.
[5] Virreira Winter S, Zychlinsky A, Bardoel BW. Genome-wide CRISPR screen reveals novel host factors required for *Staphylococcus aureus* α-hemolysin-mediated toxicity. Sci Rep 2016;6(1):24242.
[6] Inoshima I, Inoshima N, Wilke GA, Powers ME, Frank KM, Wang Y, et al. A *Staphylococcus aureus* pore-forming toxin subverts the activity of ADAM10 to cause lethal infection in mice. Nat Med 2011;17(10):1310–4.
[7] Powers ME, Kim HK, Wang Y, Bubeck WJ. ADAM10 mediates vascular injury induced by *Staphylococcus aureus* α-hemolysin. J Infect Dis 2012;206(3):352–6.
[8] Becker KA, Fahsel B, Kemper H, Mayeres J, Li C, Wilker B, et al. *Staphylococcus aureus* alpha-toxin disrupts endothelial-cell tight junctions via acid sphingomyelinase and ceramide. Infect Immun 2017;86(1):e00606-17.
[9] Reiss K, Saftig P. The "A Disintegrin And Metalloprotease" (ADAM) family of sheddases: physiological and cellular functions. Semin Cell Dev Biol 2009;20(2):126–37.
[10] Isozaki T, Rabquer BJ, Ruth JH, Haines GK, Koch AE. Rheumatism, ADAM-10 is overexpressed in rheumatoid arthritis synovial tissue and mediates angiogenesis. Arthritis Rheum 2013;65(1):98–108.
[11] Vandenabeele P, Galluzzi L, Vanden Berghe T, Kroemer G. Molecular mechanisms of necroptosis: an ordered cellular explosion. Nat Rev Mol Cell Biol 2010;11(10):700–14.
[12] Cai Z, Zhang A, Choksi S, Li W, Li T, Zhang XM, et al. Activation of cell-surface proteases promotes necroptosis, inflammation and cell migration. Cell Res 2016;26(8):886–900.
[13] Kitur K, Parker D, Nieto P, Ahn DS, Cohen TS, Chung S, et al. Toxin-induced necroptosis is a major mechanism of *Staphylococcus aureus* lung damage. PLoS Pathog 2015;11(4):e1004820.
[14] Han X, Sun S, Sun Y, Song Q, Zhu J, Song N, et al. Small molecule-driven NLRP3 inflammation inhibition via interplay between ubiquitination and autophagy: implications for Parkinson disease. Autophagy 2019;15(11):1860–81.
[15] Odegaard JI, Ricardo-Gonzalez RR, Goforth MH, Morel CR, Subramanian V, Mukundan L, et al. Macrophage-specific PPARγ controls alternative activation and improves insulin resistance. Nature 2007;447(7148):1116–20.
[16] Pineda-Torra I, Gage M, de Juan A, Pello OM. Isolation, culture, and polarization of murine bone marrow-derived and peritoneal macrophages. Methods Mol Biol 2015;1339:101–9.
[17] Wiegand I, Hilpert K, Hancock REW. Agar and broth dilution methods to determine the minimal inhibitory concentration (MIC) of antimicrobial substances. Nat Protoc 2008;3(2):163–75.
[18] Münzenmayer L, Geiger T, Daiber E, Schulte B, Autenrieth SE, Fraunholz M, et al. Influence of Sae-regulated and Agr-regulated factors on the escape of *Staphylococcus aureus* from human macrophages. Cell Microbiol 2016;18(8):1172–83.
[19] Trott O, Olson AJ. AutoDock Vina: improving the speed and accuracy of docking with a new scoring function, efficient optimization, and multithreading. J Comput Chem 2010;31(2):455–61.
[20] Murphy G. Regulation of the proteolytic disintegrin metalloproteinases, the 'Sheddases'. Semin Cell Dev Biol 2009;20(2):138–45.
[21] Fu J, Zhou M, Gritsenko MA, Nakayasu ES, Song L, Luo ZQ. *Legionella pneumophila* modulates host energy metabolism by ADP-ribosylation of ADP/ATP translocases. eLife 2022;11:11.

[22] Parker D, Prince A. *Staphylococcus aureus* induces type I IFN signaling in dendritic cells via TLR9. J Immunol 2012;189(8):4040–6.
[23] Leemans JC, Juffermans NP, Florquin S, van Rooijen N, Vervoordeldonk MJ, Verbon A, et al. Depletion of alveolar macrophages exerts protective effects in pulmonary tuberculosis in mice. J Immunol 2001;166(7):4604–11.
[24] Zuegg J, Muldoon C, Adamson G, McKeveney D, Le Thanh G, Premraj R, et al. Carbohydrate scaffolds as glycosyltransferase inhibitors with *in vivo* antibacterial activity. Nat Commun 2015;6(1):7719.
[25] Manach C, Scalbert A, Morand C, Rémésy C, Jiménez L. Polyphenols: food sources and bioavailability. Am J Clin Nutr 2004;79(5):727–47.
[26] Mullooly M, McGowan PM, Kennedy SA, Madden SF, Crown J, O' Donovan N, et al. ADAM10: a new player in breast cancer progression? Br J Cancer 2015;113(6):945–51.
[27] Maretzky T, Reiss K, Ludwig A, Buchholz J, Scholz F, Proksch E, et al. ADAM10 mediates E-cadherin shedding and regulates epithelial cell-cell adhesion, migration, and β-catenin translocation. Proc Natl Acad Sci USA 2005;102(26):9182–7.
[28] Soe YM, Bedoui S, Stinear TP, Hachani A. Intracellular *Staphylococcus aureus* and host cell death pathways. Cell Microbiol 2021;23(5):e13317.
[29] Samson AL, Zhang Y, Geoghegan ND, Gavin XJ, Davies KA, Mlodzianoski MJ, et al. MLKL trafficking and accumulation at the plasma membrane control the kinetics and threshold for necroptosis. Nat Commun 2020;11(1):3151.
[30] Yabal M, Müller N, Adler H, Knies N, Groß CJ, Damgaard RB, et al. XIAP restricts TNF- and RIP3-dependent cell death and inflammasome activation. Cell Rep 2014;7(6):1796–808.
[31] Ming D, Wang D, Cao F, Xiang H, Mu D, Cao J, et al. Kaempferol inhibits the primary attachment phase of biofilm formation in *Staphylococcus aureus*. Front Microbiol 2017;8:2263.
[32] Kaiser WJ, Sridharan H, Huang C, Mandal P, Upton JW, Gough PJ, et al. Toll-like receptor 3-mediated necrosis via TRIF, RIP3, and MLKL. J Biol Chem 2013;288(43):31268–79.
[33] Chan FKM, Luz NF, Moriwaki K. Programmed necrosis in the cross talk of cell death and inflammation. Annu Rev Immunol 2015;33(1):79–106.
[34] Ramachandran RP, Spiegel C, Keren Y, Danieli T, Melamed-Book N, Pal RR, et al. Mitochondrial targeting of the enteropathogenic *Escherichia coli* map triggers calcium mobilization, ADAM10-MAP kinase signaling, and host cell apoptosis. MBio 2020;11(5):e01397-20.
[35] Ruiz-Garcia A, Lopez-Lopez S, Garcia-Ramirez JJ, Baladron V, Ruiz-Hidalgo MJ, Lopez-Sanz L, et al. The tetraspanin TSPAN33 controls TLR-triggered macrophage activation through modulation of NOTCH signaling. J Immunol 2016;197(8):3371–81.
[36] Czaplewski L, Bax R, Clokie M, Dawson M, Fairhead H, Fischetti VA, et al. Alternatives to antibiotics—a pipeline portfolio review. Lancet Infect Dis 2016;16(2):239–51.
[37] Berube BJ, Bubeck WJ. *Staphylococcus aureus* α-toxin: nearly a century of intrigue. Toxins 2013;5(6):1140–66.
[38] Tam VC, Suen R, Treuting PM, Armando A, Lucarelli R, Gorrochotegui-Escalante N, et al. PPARα exacerbates necroptosis, leading to increased mortality in postinfluenza bacterial superinfection. Proc Natl Acad Sci USA 2020;117(27):15789–98.
[39] Reboud E, Bouillot S, Patot S, Béganton B, Attrée I, Huber P. *Pseudomonas aeruginosa* ExlA and *Serratia marcescens* ShlA trigger cadherin cleavage by promoting calcium influx and ADAM10 activation. PLoS Pathog 2017;13(8):e1006579.
[40] González-Juarbe N, Gilley RP, Hinojosa CA, Bradley KM, Kamei A, Gao G, et al. Pore-forming toxins induce macrophage necroptosis during acute bacterial pneumonia. PLoS Pathog 2015;11(12):e1005337.
[41] Wetzel S, Seipold L, Saftig P. The metalloproteinase ADAM10: a useful therapeutic target? Biochim Biophys Acta Mol Cell Res 2017;1864(11 11 Pt B):2071–81.
[42] Han X, Zhao S, Song H, Xu T, Fang Q, Hu G, et al. Kaempferol alleviates LD-mitochondrial damage by promoting autophagy: implications in Parkinson's disease. Redox Biol 2021;41:101911.
[43] Kim N, Lee HJ. Target enzymes considered for the treatment of Alzheimer's disease and Parkinson's disease. BioMed Res Int 2020;2020:2010728.